

# Shoaling guppies evade predation but have deadlier parasites

Jason C. Walsman<sup>1</sup><sup>2</sup>, Mary J. Janecka<sup>1</sup>, David R. Clark<sup>1</sup>, Rachael D. Kramp<sup>1</sup>, Faith Rovenolt<sup>1</sup>, Regina Patrick<sup>1</sup>, Ryan S. Mohammed<sup>2,3</sup>, Mateusz Konczal<sup>4</sup>, Clayton E. Cressler<sup>5</sup> and Jessica F. Stephenson<sup>1</sup>

Parasites exploit hosts to replicate and transmit, but overexploitation kills both host and parasite. Predators may shift this costbenefit balance by consuming infected hosts or changing host behaviour, but the strength of these effects remains unclear. Here we use field and lab data on Trinidadian guppies and their *Gyrodactylus* spp. parasites to show how differential predation pressure influences parasite virulence and transmission. We use an experimentally demonstrated virulence-transmission trade-off to parametrize a mathematical model in which host shoaling (as a means of anti-predator defence), increases contact rates and selects for higher virulence. Then we validate model predictions by collecting parasites from wild, Trinidadian populations; parasites from high-predation populations were more virulent in common gardens than those from low-predation populations. Broadly, our results indicate that reduced social contact selects against parasite virulence.

nprecedented infectious disease emergence among human and wildlife populations1 demands that we improve our understanding of the evolutionary ecology of parasites and pathogens (hereafter 'parasites'). A key tenet of the evolutionary theory of infectious disease is that parasite genotypes with a disadvantage in terms of higher virulence have an advantage in another trait, such as transmission<sup>2,3</sup> (or, less commonly, in the rate at which hosts recover from infection4). Parasites exploit their hosts to replicate and transmit, but increasing this exploitation harms parasite fitness by killing hosts ('virulence'), which reduces the time window for successful transmission, or the 'infectious period'5. With appropriate curvature, this trade-off should result in stabilizing selection for intermediate virulence<sup>6-9</sup> instead of directional selection for minimum or maximum virulence. Theory predicts that various ecological mechanisms can shift the costs and benefits of exploitation, altering virulence evolution along a trade-off<sup>10-13</sup> and host disease outcomes;<sup>3,8,14,15</sup> but empirical evaluation of such critical, eco-evolutionary shifts remains scant<sup>3,16,17</sup>.

Predation is one such mechanism that can theoretically select for higher or lower virulence<sup>3,10,12</sup> through multiple pathways (we highlight four in Fig. 1). Predation directly increases overall host mortality, selecting for faster exploitation of and transmission from infected hosts before the host dies<sup>10,11,17</sup> (pathway 1 in Fig. 1). Alternatively, predation can select for lower virulence. Predation typically lowers the density of infected hosts, reducing the per host rate at which new infections arise ('force of infection'), and this lower force of infection reduces infections with multiple parasite genotypes ('multiple infections'). Multiple infections often create within-host competition (unlike in<sup>18</sup>), so more multiple infections favour higher virulence<sup>12,16</sup> (pathway 2 in Fig. 1). In addition to these consumptive effects, predators can also affect host traits<sup>19</sup>, non-consumptively shifting how hosts interact with their parasites<sup>20–22</sup>, and probably virulence evolution. One example is host grouping, a common

defence<sup>23</sup>, which effectively decreases predator-induced mortality<sup>24</sup>, potentially selecting for lower virulence (pathway 3 in Fig. 1). However, grouping rate also increases the host-host contact rate, increasing the force of infection, so host grouping could increase multiple infections and therefore select for higher virulence<sup>13,16,25</sup> (pathway 4). Both consumptive and non-consumptive effects of predation act simultaneously in natural communities<sup>21</sup>, but their relative importance for selection on parasite virulence lacks empirical and theoretical clarification.

Here we elucidate how predators affect virulence using theory and data from Trinidadian guppies, *Poecilia reticulata* and their *Gyrodactylus* spp. ectoparasites (Fig. 2). These parasites transmit directly during contact and reproduce directly on the host. Persistent, natural variation in predation risk drives population-level variation in guppy grouping ('shoaling rate')<sup>26–28</sup>, probably influencing parasite transmission<sup>29–32</sup>; high-predation populations shoal more and suffer higher *Gyrodactylus* spp. infection prevalence<sup>30,33,34</sup>.

We leveraged this system to test how the consumptive and non-consumptive effects of predation drive virulence evolution (Extended Data Fig. 1). First, we tested for the commonly assumed virulence-transmission trade-off using previously published data and new data from our transmission rate experiment. We connected this to new data on infection intensity and infected host death rate for parasite lines from our line traits experiment. Second, we tested for the presence of multiple infections using a field survey of coinfection rates in wild populations (Extended Data Fig. 2). Third, we used laboratory and field measurements to parametrize a model with selection on host and parasite phenotypes interacting with host and parasite densities ('eco-coevolutionary model'). We used many previously published datasets, our trade-off and new data from field surveys of shoaling rate and infection prevalence ('training data'). Fourth, we derived key model predictions for how predation affects virulence and elucidated the model mechanism of shoaling

<sup>&</sup>lt;sup>1</sup>Department of Biological Sciences, University of Pittsburgh, Pittsburgh, PA, USA. <sup>2</sup>Department of Life Sciences, University of the West Indies, St. Augustine, Trinidad and Tobago. <sup>3</sup>Biology Department, Thompson Biology Lab, Williams College, Williamstown, MA, USA. <sup>4</sup>Evolutionary Biology Group, Faculty of Biology, Adam Mickiewicz University, Poznań, Poland. <sup>5</sup>School of Biological Sciences, University of Nebraska, Lincoln, NE, USA. <sup>™</sup>e-mail: walsmanjason@gmail.com

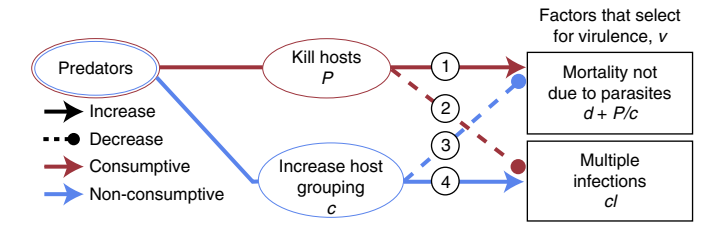


**Fig. 1** | Predators alter selection on virulence through consumptive and non-consumptive pathways. The consumptive (red) and non-consumptive (blue) effects of predation simultaneously act to increase (solid, triangular arrows) and decrease (dashed, rounded arrows) factors that select for higher virulence. Mortality that is not due to parasites is d + P/c, where d is background mortality, P is predation and c is host grouping rate or 'shoaling rate'. The force of infection for multiple infections is proportional to cl, where l is the density of infected hosts. Created with biorender (https://www.biorender.com).

rate and multiple infections. The model supported the importance of shoaling rate compared with alternative model considerations such as selective predation or variation in host resistance (Extended Data Fig. 3). Fifth and finally, we tested model predictions with the mean virulence of wild-collected *Gyrodactylus* spp. parasites from four focal populations ('validating data' found from the line traits

experiment). These assays disentangled parasite traits from host defences by using common garden conditions.

#### Results

Transmission-virulence trade-off, mediated by parasite intensity. To confirm the common assumption about parasite evolution and provide training data for our model, we searched for a virulence-transmission trade-off among Gyrodactylus spp. lines by measuring disease traits on individual hosts. First, we conducted a transmission rate experiment and found that measured transmission rate from a donor to recipient host increased in a saturating manner as measured intensity (measured at day of transmission) increased (Fig. 3a;  $\beta = 6.08 \times 10^{-3}$  intensity<sup>0.138</sup>; generalized linear model (GLM) N=101,  $P=3.48\times10^{-5}$ , r=0.35; Methods provide more details). This pattern did not differ across this experiment and a previously published one35 using different, domestic parasite lines (all lines were isolated from commercial guppies; line effect: GLM, N=101, P=0.596, effect size  $(\varphi)=0.12$ ). Our transmission rate experiment included a coinfection treatment, so this result suggests that the intensity-transmission rate relationship is similar across parasite genotypes and is not affected by coinfection. Its saturating shape is consistent with probabilistic expectations; transmission rate  $(\beta)$  is shoaling rate (c) multiplied by transmissibility given contact (*T*). If each of *n* worms has an independent chance of transmission given contact (y), then transmission rate follows this saturating relationship:  $\beta = c(1 - (1 - y)^n)$ .

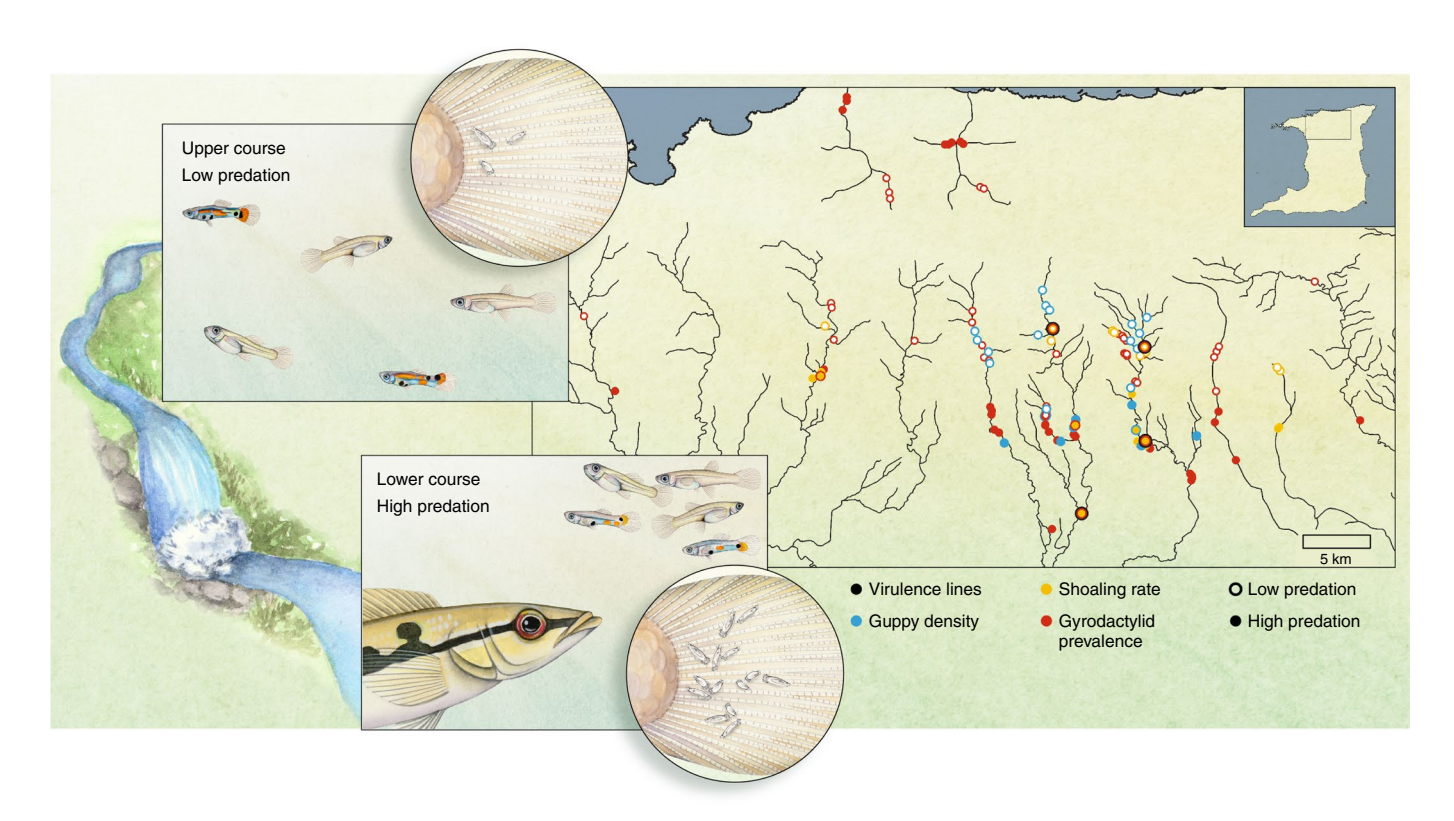


**Fig. 2 | Natural guppy populations differ in predation, driving evolutionary divergence in shoaling rate.** Waterfalls divide upper- and lower-course guppy populations, preventing upstream migration of large piscivores. Natural populations have therefore evolved under different predation regimes, replicated across rivers. Shoaling rate differences apparently drive population-level differences in transmission rate of <sup>30-32</sup>—and thus selection on the virulence of—their highly prevalent, directly transmitted monogenean ectoparasites *Gyrodactylus* spp. The map shows locations and data types that parameterized and validated model quantities (Methods). Points are combined when multiple data types were collected from one site; for example, a black, red, yellow, unfilled point shows that virulence, shoaling rate and prevalence were collected from a low-predation site. Virulence lines formed part of our line traits experiment. All other data types shown here were a mixture of previously published data and our field surveys of shoaling rate and prevalence. To focus on the effects of predation, we used data from a river if that data type was available in both low- and high-predation populations for that river. Credit: Julie Johnson.

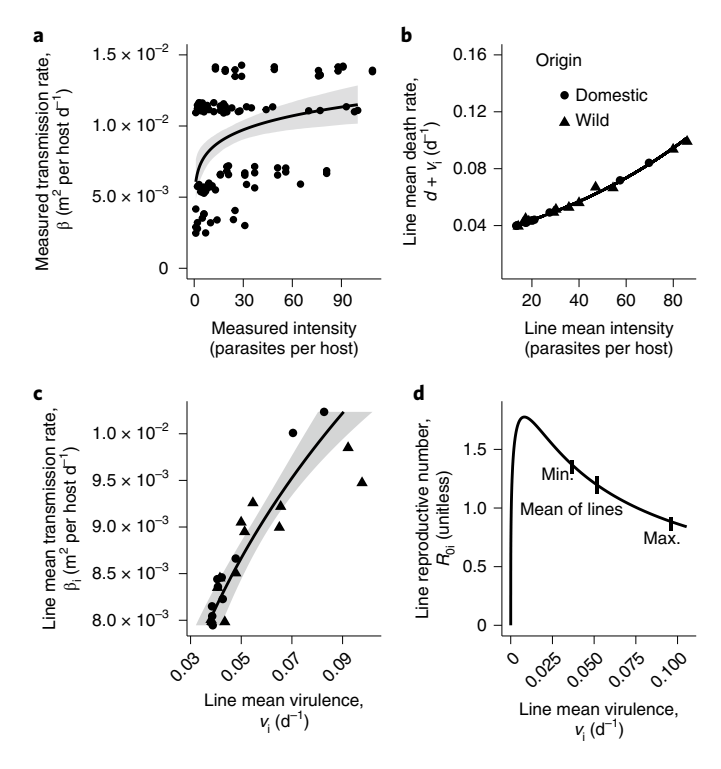


Fig. 3 | Infection intensity links transmission rate and virulence with a stabilizing trade-off. a, Across four parasite lines, measured transmission rate increased with measured infection intensity. Points are transmission events (jittered vertically) and measured intensity from our transmission rate experiment. **b**, Across 22 parasite lines in our line traits experiment, those with higher line mean intensity (probably related to parasite growth rate) induced higher line mean host death rate ( $d + v_i$ , a measure of virulence; back transformed partial residuals). c, Using all measured intensities for each line, we predicted transmission rates at each measured intensity using the relationship in a. We then took the line mean predicted transmission rate for a line to plot against line mean virulence. Points in b,c are line mean traits ('domestic' (circles) or 'wild' (triangles)). In a-c, bands are 95% confidence intervals, and curves are GLM fits.  $\boldsymbol{d}$ , The curvature in  $\mathbf{c}$  maximizes  $R_{0i}$  at intermediate transmission rate/virulence. Minimum (Min.), mean, and maximum (Max.) virulence of lines shown. Created with biorender (https://www.biorender.com).

Second, in our line traits experiment, we measured worm parasites per fish (intensity) and the death rate of infected hosts for 22 laboratory-maintained lines (including three of four from Fig. 3a; Methods provide detail on determining that lines were genetically distinct). Lines differed in the line mean intensity they attained (analysis of variance (ANOVA), N=1,171,  $P=9.36\times10^{-25}$ , effect size  $(\eta^2) = 0.13$ ), probably owing to faster exploitation of and reproduction on individual hosts; higher line mean intensity corresponded to higher line mean death rate of infected hosts (Fig. 3b; GLM, N=22, P=0.008, r=0.49). Note that laboratory intensities were comparable to those observed in the field (Supplementary Fig. 1). Across line mean intensities, domestic lines imposed less line mean death (GLM, N=22,  $P=1.24\times10^{-4}$ , r=0.63; domestic=0.016 versus wild=0.052 at mean of line mean intensities). We used a back transformed, partial residual death rate to control for the non-focal predictor (line origin: Fig. 3b shows the relationship as if all lines were wild) so that we could determine the relationship relevant to wild parasites (all results are very similar if instead we set all lines as domestic).

Third, we found the line mean predicted transmission rate, given measured intensities and the transmission–intensity relationship

in Fig. 3a. Because there is no evidence that the intensity–transmission rate relationship changes with infection duration<sup>35</sup>, we took measured intensities throughout the course of infection and mapped each onto a predicted transmission rate. We found that the line means of these predicted transmission rates traded off with the line means of virulence (we get virulence for each line,  $v_i$ , from infected host death rate,  $d+v_i$ , given  $d=1.30\times10^{-3}$  d<sup>-1</sup>). It is arbitrary whether we consider  $\beta_i$  as a function of  $v_i$  or vice versa, as the likely underlying mechanism for both is intensity; Fig. 3a predicts how parasite lines that attained higher intensity benefit from higher transmission rate but higher virulence shortened their infections, on average (Fig. 3b, linked together in Fig. 3c).

The curvature of this trade-off indicated stabilizing selection on virulence (seen as saturating curvature in Fig. 3c; GLM fit:  $v_i = 1.38 \times 10^6 \ \beta_i^{3.61}$ ;  $v_i$  and  $\beta_i$  are average traits for a line). Bootstrapping parasite lines included in the analysis showed this curvature was significant (found in all 10<sup>4</sup> bootstrapped samples) and Akaike information criterion (AIC) indicates a better fit to the data than for a linear model ( $\Delta$ AIC=13.3). Theory predicts that the trade-off curvature leads to optimal parasite fitness at intermediate transmissibility ( $\beta_i = cT_i$ , where c is the host shoaling rate and  $T_i$  is a line's transmissibility) and virulence (Fig. 3d; parasite reproductive number is  $R_{0i} = cT_iS/(d+v_i+y)$  for pure infections where we use reasonable values of S = 10 susceptible host m<sup>-2</sup> and  $\gamma = 0.020 \,\mathrm{d}^{-1}$ , Table 1). While mixed-stock guppies in our common garden assay may differ substantially from local, wild hosts in ways that could raise or lower effective virulence, we had two reasons to expect line means of virulence to fall to the right of this optimum: first, higher background mortality in wild rather than laboratory guppies means this optimum occurs at higher virulence in wild rather than laboratory guppies; second, multiple infections (common in the wild, Extended Data Fig. 2) select for higher virulence than would optimize  $R_{0i}$  of pure infections<sup>12</sup>. Thus, our stabilizing trade-off and location of lines on that trade-off is very consistent with typical evolutionary theory.

Model predicts deadlier parasites for more social hosts. Our eco-coevolutionary model provides some general insight and much more insight when parametrized by our training data from our focal system. As a first general insight, it demonstrates that the net selective effect of predation, shoaling rate or other ecological factors on virulence evolution depends only on their effect on the rate at which infections are lost to mortality or multiple infections (inverse of infectious period; Supplementary Note for proof). Second, the model shows that shoaling rate evolves to balance predator-induced mortality against parasite-induced mortality. When predation increases, hosts evolve higher shoaling rate, increasing transmission rate. When parasites are more abundant and virulent, hosts evolve lower shoaling rate to prevent infection. For some parameter values, higher virulence can select for higher shoaling rate if parasites become so virulent that the density of infected hosts and force of infection decline strongly (Extended Data Fig. 4).

When parametrized with empirical data from the guppy-Gyrodactylus spp. system, the model complexity resolves into one dominant pathway: predation increases coevolutionarily stable shoaling rate, multiple infections and thus virulence (Fig. 4; strength of pathways from Fig. 1: pathway 1=0.131, pathway 2=-0.166, pathway 3=-0.063, pathway 4=1.18 with units of change in transmissibility per change in predation; Supplementary Note for derivation). When predators only have consumptive effects on predation (that is, hosts do not evolve; Fig. 1: pathways 1 and 2), predation decreases prevalence and virulence (grey curves in Fig. 5a-e; presence/absence of parasite evolution has little effect on grey curves). However, as hosts evolve higher shoaling rate in response to predation (Fig. 5a), predation also increases prevalence (bl ack curve in Fig. 5b) in all tested parameter sets (sensitivity

Symbol	Meaning	Value and/or units	Training value
S	Susceptible host density	hosts m <sup>-2</sup>	
I	Infected host density	hosts m <sup>-2</sup>	
R	Recovered host density	hosts m <sup>-2</sup>	
$(S+I+R)_{Low}$	Total host density, low predation	5.61 hosts m <sup>-2</sup>	8.19
$(S+I+R)_{Hi}$	Total host density, high predation	4.69 hosts m <sup>-2</sup>	4.68
$(S+I+R)_{Hi}/(S+I+R)_{Low}$	Host density ratio	0.837 hosts m <sup>-2</sup>	0.571
p	Prevalence: $p = I/(S + I + R)$	Unitless	
$p_{Low}$	Prevalence, low predation	0.288	0.311
$p_{Hi}$	Prevalence, high predation	0.400	0.394
$p_{Hi}/p_{Low}$	Prevalence ratio	1.39	1.27
a	Maximum host per capita fecundity	0.106 d <sup>-1</sup>	a = 0.106
c	Host shoaling rate	$1.7-5.5{\rm m}^2{\rm per}{\rm host}{\rm d}^{-1}$	
c <sub>Hi</sub> /c <sub>Low</sub>	Shoaling rate ratio	2.23	1.93
C <sub>1</sub>	Scaling parameter for shoaling rate	1 m² per host d <sup>-1</sup>	
d	Background host death rate	$1.30 \times 10^{-3} d^{-1}$	$d = 1.41 \times 10^{-3}$
k <sub>1</sub>	Trade-off parameter: virulence with transmissibility=1	1.38×10 <sup>6</sup> d <sup>-1</sup>	See text
k <sub>2</sub>	Trade-off parameter: exponent	3.61	See text
D	Predation regime	$7.4-33.0 \times 10^{-3} d^{-1}$	
$(d + Pc\sqrt{c} + pv)_{low}$	Overall host mortality, low predation	0.011 d <sup>-1</sup>	0.011
$(d+Pc_{1}/c+pv)_{Hi}$	Overall host mortality, high predation	0.026 d <sup>-1</sup>	0.026
$(d + Pc \sqrt{c} + pv)_{Hi} / (d + Pc \sqrt{c} + pv)_{Low}$	Overall host mortality ratio	2.46	2.47
9	Density dependence of host fecundity	$0.017m^2$ per host $d^{-1}$	
Т	Transmissibility given contact	6.2-8.81×10 <sup>-3</sup>	Not trained
(cT) <sub>Low</sub>	Transmission rate, low predation	$0.015m^2$ per host $d^{-1}$	0.014
сТІ	Force of infection	$d^{-1}$	Not trained
V	Mortality virulence	0.015-0.053 d <sup>-1</sup>	Not trained
$y_{Low}$	Virulence, low predation	$0.020d^{-1}$	Validated: 0.021
V <sub>Hi</sub>	Virulence, high predation	$0.044d^{-1}$	Validated: 0.041
Z	Rate of waning of host immunity	$0.033  d^{-1}$	z = 0.033
γ	Infected host recovery rate	$0.020d^{-1}$	y = 0.033
σ	Probability of successful superinfection given transmission	1.21	

Italics indicate state variables or parameters values. Training values may be for a parameter, an output or outputs related to a parameter or output. Training values were used in the model fitting and their sources are provided. Low/high predation indicates predation regime. Values result from the model training. Note that the model was not trained with evolved virulence data but instead validated against it. Methods provide sources of training values.

analysis in Methods). Increasing predation increases overall host mortality and reduces host density, particularly when hosts evolve (Fig. 5c). Further, most of the increase in mortality (76%) with predation is due to increased parasite-induced mortality (prevalence×virulence), rather than increased predator-induced mortality (Extended Data Fig. 5; robust to parameters: Supplementary Fig. 2). Higher shoaling rate increases the force of infection (and thus multiple infections), selecting for higher parasite intensity and virulence (Fig. 5d,e; note intensity was not modelled directly but back calculated from virulence according to Fig. 3b); in all parameter sets, higher predation increased virulence. Importantly, predators increase virulence through their non-consumptive effects on shoaling rate (across parameter sets, Supplementary Fig. 2).

**Model fits training data and predicts validating data.** The model's eco-coevolutionary outcomes successfully fit training data

from our collections and the literature (Fig. 5a-c,f-h; Table 1). High-predation fish spent more time shoaling in our field survey of shoaling rate (generalized linear mixed model (GLMM), N=68, P=0.006, r=0.32) and across population estimates extracted from the literature (GLMM, N=22, P=8.31×10<sup>-4</sup>, r=0.58; Fig. 5f). This helps explain why high-predation populations suffered higher parasite prevalence across multiple rivers, sites and years (GLMM, N=107, P=0.025, r=0.21; Fig. 5g). Higher levels of predation and parasitism may depress host density (though not significantly so; GLMM, N=23, P=0.140, r=-0.29; Fig. 5h). Overall, the model fit the training data reasonably well, with an average relative error of 10.5% per fitted quantity (shown in Fig. 5a-c,f-h and Table 1).

Alternative models do not fit the data as well, bolstering confidence in our focal eco-coevolutionary model. A model without host evolution (only consumptive effects of predators) fits the data poorly (relative error of 15.2% per fitted quantity, Supplementary

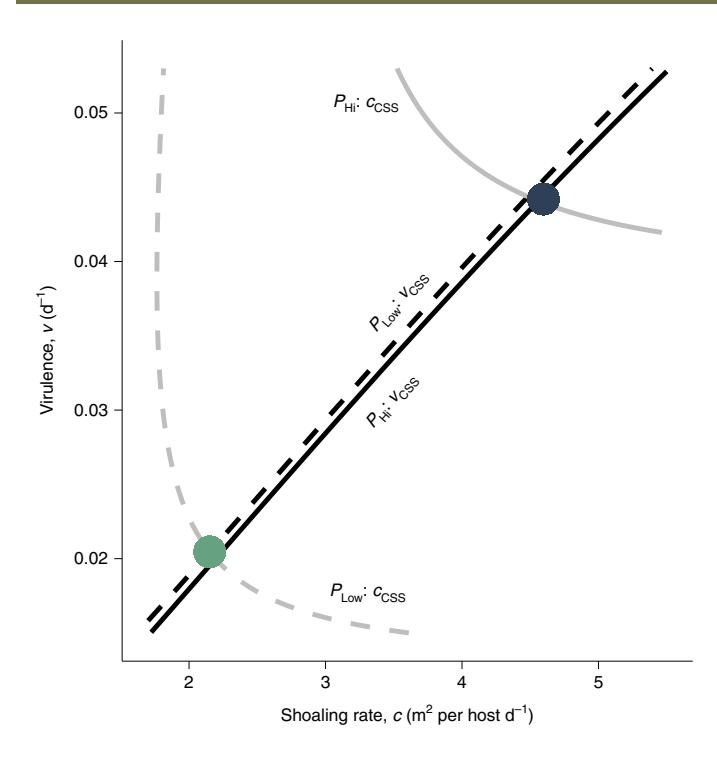


**Fig. 4 | Predation drives increased shoaling rate and virulence in the eco-coevolutionary model.** Curves give the CSS for parasite ( $v_{\text{CSS}}$ , black) or host ( $c_{\text{CSS}}$ , grey) evolution at predation levels fitted to correspond to natural populations ( $P_{\text{Low}}$ , dashed, or  $P_{\text{Hi}}$ , solid). Parasites evolve higher virulence with higher shoaling rate. The consumptive effects of predation have little net effect on evolved virulence. Hosts evolve lower shoaling rate with increasing virulence (grey curves move towards lower c as v increases). Predation substantially increases  $c_{\text{CSS}}$ . Host and parasite curves intersect at coevolutionarily stable points (green and blue points). As predation increases (from green point to blue point), coevolutionarily stable shoaling rate ( $c_{\text{coCSS}}$ ) and virulence ( $v_{\text{coCSS}}$ ) increase.

Fig. 3) despite having an additional free parameter (shoaling rate, which is not set by coevolution in this alternative model). A different alternative model fits an exponent governing how effectively shoaling protects from predation (this exponent equals 1 in our focal model), but the miniscule shift in model fit (relative error improves from 10.4% to 10.1%, Supplementary Fig. 3) does not justify the additional free parameter. Accounting for model complexity, our focal model provided the best fit to the training data, and of the three models it thus likely best captures the consumptive and non-consumptive effects of predation.

We tested the focal model's trained predictions against the average traits found for our focal populations in our line traits experiment. We quantified the traits of 18 parasite lines isolated from the focal wild populations maintained in the lab under common garden conditions for 65 days. Lines from high-predation populations attained higher intensity on infected, mixed-stock hosts (GLMM, N=425, P=0.028, r=0.11; Fig. 5i) and induced higher death rate (GLMM, N=216, P=0.029, r=0.15; Fig. 5j). The two parasite species, G. turnbulli (11 known lines) and G. bullatarudis (three known lines) did not differ significantly in intensity (GLMM, N=345, P = 0.098, r = 0.09) or virulence (GLM, N = 177, P = 0.345, r = 0.07; unlike<sup>36</sup>). Restricting the analysis for Fig. 5j to G. turnbulli found marginally higher intensity (GLM, N=208, P=0.076, r=0.12) and significantly higher virulence in high-predation populations (GLM, N=102, P=0.009, r=0.25). The overall quantitative match between the model-predicted mortality and our empirical results supports our model's inferences (d+v in the model versus mean of d+v back transformed partial residuals: low predation 0.020 versus 0.021; high predation: 0.044 versus 0.041). We compared theoretical predictions to partial residuals to control for non-focal predictors in the statistical model, especially duration of parasite maintenance in the laboratory, to obtain the most biologically relevant estimate of virulence. Our theoretical model makes this prediction based on higher shoaling rate increasing multiple infections, which seem more frequent in high-predation populations on a similar scale to shoaling rate (shoaling rate ~2 times higher and we find coinfection ~3 times higher in high predation; Extended Data Fig. 2). Despite the encouraging match between the model expectations and coinfection data, we treat this result with caution due to low sample sizes in terms of number of fish and worms genotyped per fish (Extended Data Fig. 2).

The model–data agreement on evolved virulence aids model—data agreement on how mortality changes across predation regime. In our model, 76% of the increased mortality across predation regime is increased parasite-induced mortality while increased predator-induced mortality accounts for 24%. For comparison, the difference in mortality between low and high-predation populations estimated from a mark–recapture experiment<sup>37</sup>, combined with our estimates of *Gyrodactylus* spp. prevalence and virulence ( $p_{\rm Hi}\nu_{\rm Hi}$ – $p_{\rm Low}\nu_{\rm Low}$ ) across these populations, indicate that parasitism explains 64% of the mortality difference while predation may account for the remaining 36%.

#### Discussion

Our theoretical–empirical approach clarifies that predation drives the evolution of parasite virulence by increasing the host shoaling rate. As a result, shoaling in response to increasing predation pressure leads to parasite-induced mortality rising more than that induced by predators. In contrast to these strong non-consumptive effects, we found that the consumptive effects of predation are small, balance one another out and barely alter virulence evolution. To our knowledge, our study is the first to model the non-consumptive effects of predation on virulence evolution. Further, we used data to train and test a model that infers and compares the strength of consumptive and non-consumptive effects in natural populations. We discuss key emergent patterns.

Theory shows that shoaling rate drives virulence evolution through multiple infections. Without multiple infections, shoaling decreases predator-induced mortality and thus selects for decreased virulence<sup>38</sup>. With multiple infections, we and others<sup>13</sup> find that increased grouping rate selects for higher virulence. Empirically, we do not know of previous tests of the effect of host–host contact rate on virulence evolution, but our result is analogous to more host dispersal<sup>15,39,40</sup> or parasite founder diversity<sup>14</sup>, selecting for higher host exploitation through high local parasite diversity<sup>41</sup>.

We assayed parasite traits using infections on mixed-stock, wild-type guppies; this approach allowed us to draw robust conclusions about parasite evolution but leaves untested how host defences, other than shoaling rate, may affect disease dynamics in natural communities. Thus far, guppy defences against parasites have not been robustly characterized across predation regime. Illustrative data suggest that in our focal Guanapo river (experimental test<sup>42</sup>), and perhaps more generally (field surveys30,33), guppies from low-predation regimes are better defended against Gyrodactylus spp. Low-predation guppies may be better able to evolve in response to Gyrodactylus spp. and, due to their slower life histories<sup>43</sup>, may face stronger selection for parasite defence44; they need not balance this investment with defence against predators<sup>24</sup>, and sexual selection for Gyrodactylid resistance<sup>45</sup> is more effective in the absence of predators<sup>46</sup>. However, in our focal Aripo river, low-predation guppies appear less resistant than high-predation guppies (experimental test<sup>47</sup>). Despite this apparent difference between our focal rivers, our measured virulence matched our model predictions for both,

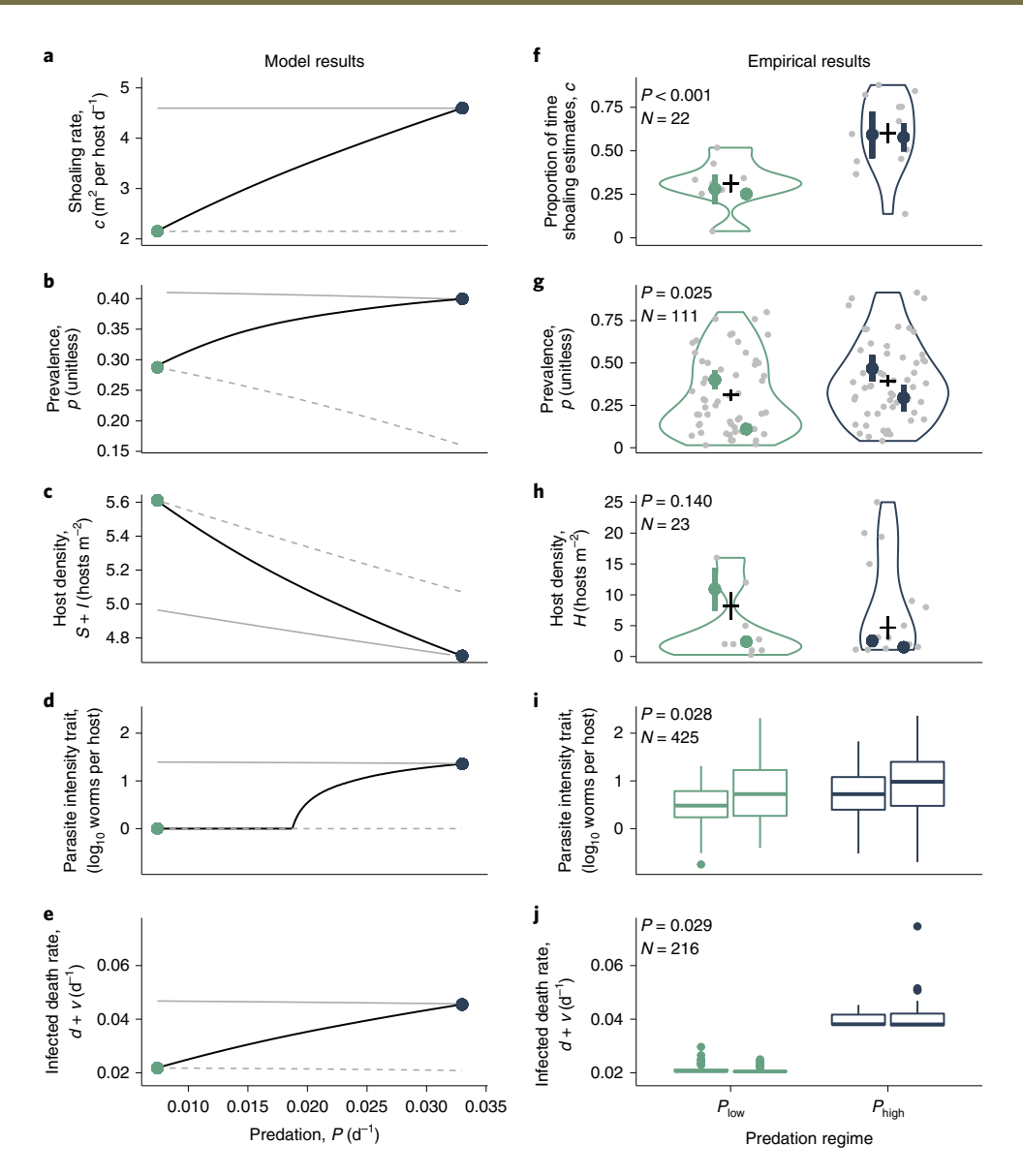


**Fig. 5 | Predation increases shoaling rate and thus selects for higher virulence. a-e**, Model results. Black curves: eco-coevolution (connecting Fig. 4 coloured points). Grey curves: no host evolution with shoaling rate set high (solid) or low (dashed). **f-h**, Empirical training data from previously published data and our field surveys. Horizontal segments: predation regime means. Grey points: one river/regime/year mean. Coloured points: one focal river/ predation regime mean (Aripo left of Guanapo). Vertical bars: standard errors. Training data: violins. **i,j**, Validating data from our line traits experiment: box plots (back transformed partial residuals; centre line, median; box limits, first and third quartiles; whiskers, 1.5× interquartile range; points, outliers). *P* values for the effect of predation regime and sample sizes (*N*) provided; all statistical tests here were generalized linear mixed models. Shoaling increased with predation (**a,f**); prevalence increased with predation (**b,g**) while host density decreased non-significantly (**c,h**); parasite intensity (note, we do not model intensity lower than log<sub>10</sub>(1 worm) = 0) (**d,i**) and virulence increased with predation (**e,j**).

suggesting the patterns we observe may be robust to population-level differences in host defences (as the model suggests, Extended Data Fig. 3). Because of multiple infections, host resistance selects for higher and lower virulence through different pathways, providing little net effect. Thus, our theoretical and empirical (common garden) techniques enable us to disentangle parasite virulence from host immunological defences in this case. However, host behavioural and immunological defences may often coevolve critically with parasite virulence in natural communities, posing an outstanding and complex theoretical and empirical challenge.

The importance and implications of predation and social parasite transmission, evident from our model and data, may hold across directly transmitted parasites of group-living hosts<sup>48</sup>. Predators drive defensive group living in animals across taxa<sup>23</sup>,

which can increase parasitism, creating ecological and evolutionary feedbacks between host sociality and parasites<sup>48,49</sup>. Parasites evolve along virulence–transmission trade-offs in systems ranging from viruses of humans<sup>6,9</sup>, bacterial pathogens of birds<sup>7</sup>, protozoan pathogens of insects<sup>8</sup> and our monogenean fish ectoparasite. Multiple infections are common for many parasites, allowing the simple mechanism of competition for within-host resources to select for higher virulence<sup>16</sup>. Thus, diverse systems likely meet the essential assumptions of our model; predators may frequently shift the antagonistic interplay of host sociality and parasite virulence, driving hosts into the arms of more virulent parasites. Conversely, these results also indicate that social distancing may select for lower virulence when parasites exhibit multiple infections and a virulence–transmission trade-off (for example, influenza A virus<sup>6,50</sup>). Host

NATURE ECOLOGY & EVOLUTION ARTICLES

behaviour that reduces contact may thus effectively control both the spread and virulence evolution of pathogens and parasites.

#### Methods

Molecular methods. We used molecular methods to determine coinfection rates and ensure our lines were genetically distinct. We used two methods of molecular species identification for individual parasites; we sequenced the mitochondrial COII gene for a subset of domestic lines established before March 2020, and we used a newly developed restriction enzyme assay for wild and domestic lines established after March 2020 (Supplementary Note). To prevent disrupting data collection, sample collection was restricted to already-dead hosts, stored in 70% EtOH. This conservative precaution meant we were unable to collect useable samples from some of our parasite lines.

We developed panels of single nucleotide polymorphisms for *G. turnbulli* and *G. bullatarudis* to determine non-sibling genotypes. Genotypes were called using Fluidigm single nucleotide polymorphism genotyping analysis software. A subset of individuals was re-genotyped to identify and remove error-prone loci and estimate error rates (the proportion of mismatches to matches for re-genotyped loci). Loci that amplified consistently and with score calls greater than 90% were selected for use in the analysis. This resulted in a total of 140 variable loci for *G. turnbulli* (error rate 1.5%) and 83 loci for *G. bullatarudis* (error rate 2%) across all populations. However, due to substantial local variation in informative loci, the total number of loci used for each source population varied (Supplementary Table 1). The resulting multilocus genotypes were assessed using GENALEX 6.502 to estimate the fraction of multi-genotype infections at six sites across Trinidad including our four focal populations (low- and high-predation in the Aripo and Guanapo rivers) and to assess the genotypes of the established line.

As a conservative estimate, two individuals were considered to have different genotypes if they varied in at least 50% of the total variable loci from a given source population (ensuring they were non-siblings, Supplementary Information provide further details on methods). This applied both to determining that our lines were different genotypes and finding the frequency of multiple infections in the field survey of coinfection rates. Genotyping a subset of our lines (13/22, based on sample availability) found no sibling lines (all pairs within populations differed at ≥16 loci, representing at least half of all variable loci for each source population, Supplementary Table 1). In finding the frequency of multiple infections, we genotyped worms from fish with at least two worms and accounted for the proportion of fish with only one worm, estimated for each site from our 2020 survey and Stephenson et al. <sup>30</sup>. See Supplementary Note for more details on our molecular methods.

Parasite experiments. Line establishment and maintenance. We established parasite lines by transferring a single worm to an uninfected host from our mixed, laboratory-bred stocks descended from wild populations. Each founding worm was obtained from a single guppy either from a commercial supplier ('domestic' lines) or wild-caught in Trinidad ('wild' lines from Caura, Aripo, Guanapo and Lopinot rivers in Caroni drainage). Wild-caught adult guppies (~50/population) were shipped from Trinidad to the University of Pittsburgh in March 2020 (Animal use ethics statement). We established 43 parasite lines (18 domestic and 25 wild comprised of 10 from low-predation populations and 15 from high predation). Different lines were included in different analyses, as explained below. Wild lines were maintained under common garden conditions for 65 days (some domestic lines were maintained in the lab much longer) on groups of three to six guppies. We added uninfected fish to each line as required to replace those that either died or were found parasite-free during twice-weekly screening of all fish in each line under anaesthetic (tricaine methanesulfonate 'MS222'; 4 gl<sup>-1</sup>) using a dissecting microscope. During these screens, we recorded the number of parasites infecting each fish. Each line was housed in a single 1.81 tank on a recirculating system (Aquaneering Inc.; 121:12D; 24°C). Recirculated water passes through fine foam, sand and ultraviolet filters before re-entering other tanks; individual parasites cannot transmit between lines, as supported by our genotyping.

Transmission rate experiment. We estimated transmission rate by re-analysing data from Stephenson et al.35 and conducting a similar new experiment (our transmission rate experiment). We used only one transmission event per fish from Stephenson et al.35 to simplify error structure; to keep a more comparable range of intensities, we used the second transmission event from those of Stephenson et al.'s  $^{\rm 35}$  fish that had two transmission events. Regardless, the transmission intensity relationship seems to hold across a range of intensity regardless of the day of transmission (Supplementary Fig. 4). Donor fish received an infection of one parasite line or multiple infection and were individually housed in 1.81 tanks (donor fish received line A, B, C or A and B); no lines in the new experiment were used by Stephenson et al.35. To infect donor fish, culture fish were euthanized with an overdose of MS222 or pithing (pithed fish were washed several times with clean water until oil from the injury sight was no longer observed); the culture fish was placed in close proximity with the anesthetized donor fish under a dissecting microscope until two individual parasites had transmitted. We added a parasite-naïve recipient fish on day 8 of the donor's infection and screened both fish for infection every 24 h.

We calculated a measured transmission rate from the number of days until successful infection of the recipient and the corresponding measured intensity as the number of worms on the donor fish on the day of transmission, following Stephenson et al.  $^{35}$  (total n=101 transmission events). Worm numbers changed slowly on the scale of the number of days until successful infection. In these assays,  $dS/dt=-cT_i IS$  (c is shoaling rate,  $T_i$  is the transmissibility of parasite line i, I is infected host density and S is susceptible host density) so susceptible hosts follow an exponential decay pattern; thus, mean time until infection is  $1/(cT_i I)$ . If days until transmission are D, then the measured transmission rate estimated by a given transmission event is  $cT_i=1/(DI)$ . On the basis of the area of enclosures, infected host densities were I=88.5 hosts  $\rm m^{-2}$  for Stephenson et al.  $^{35}$  and I=72.0 hosts  $\rm m^{-2}$  for the follow-up experiment.

We fit these measured transmission rates to  $\log_{10}$  measured intensities with parasite line (line A, B, C, or coinfection of lines A and B) as a fixed effect using a generalized linear model with a Gamma error family and log link function. Parasite line was non-significant, so we refit the model without parasite line (P value for intensity reported from this model; all P values represent two-sided, Type II Wald chi-square or F tests for this and other methods). Effect sizes are  $\eta^2$  for ANOVA with only two levels of predictors,  $\varphi$  for ANOVA with more than two levels of predictors or partial correlation coefficients, r, for other analyses. For all analyses, we provide the code, output and validation of the model fit in the Supplementary Information.

Because transmission rate was calculated from days until transmission and we checked for transmission every 24 h, the fastest transmission rate we could measure corresponded to transmission in one day. In theory, this measurement constraint could create a saturating relationship of measured transmission rate as a function of measured intensity if even very high intensities still corresponded to only this maximum measured transmission rate. To test this, we refit this statistical model to a subset of the data restricting to low measured intensities (<50) but found the same suturing curve with quantitatively very similar parameter fits. Thus, our saturating relationship in Fig. 3a is not created by strictly constraining to a maximum transmission rate even at very high intensities.

Line traits experiment. We also assayed intensity and death rate in our line traits experiment. For measured intensity (probably related to within-host growth rate), we counted the number of parasites on each host at each date (one measured intensity). We estimated the per capita host death rate from the number of fish found dead divided by the number of infected fish in the tank at the previous observation time point and the days between observations (one observation; 79% of observations were  $3\pm1$  days after the previous one).

When determining average traits for a line, we included only lines maintained in the laboratory for more than 30 days (n = 22; 10 domestic, 12 wild lines, including 1-4 lines from each of the four focal populations). We used an ANOVA to determine whether lines differed significantly in log measured intensities (1,171 measured intensities for the 22 parasite lines, at least 25 for each line). We modelled line mean death rate of infected hosts (344 observations and at least 13 for each line) as a function of line mean intensity and line origin (wild versus domestic) with a beta error family and logit link function. We estimated line mean virulence (v) by subtracting background death rate (Table 1) from partial residuals of line mean death rate (to get  $\nu$  from  $d+\nu$ ). We used partial residuals of line mean death rate back transformed onto the response scale to control for non-focal predictors (here, line origin) and find the relationship for wild parasites. We found line mean predicted transmission rate by mapping the individual measured intensities for each line onto the relationship observed between measured intensity and measured transmission rate in the experiments described above (Fig. 3a); we took the mean of these predicted transmission rates to get the line mean predicted transmission rate for each line. With line mean predicted transmission rates and line means of virulence, we examined the relationship between them using a generalized linear model of virulence with Gaussian error distribution and log link function as a function of natural log transmission rate. The statistical model was free to fit a positive (exponent>1), neutral (exponent=1), or negative curvature (exponent <1) to these data. We bootstrapped this fit by sampling lines to include in the analysis from the 22 parasite lines with replacement to determine how often the exponent was more than one (indicating a stabilizing curvature).

To examine the patterns in Fig. 5i,j, we used our measured intensities and infected host death rates, (calculated as above from our line traits experiment) as response variables in GLMMs. These traits were assayed from parasites collected from low- and high-predation populations of our focal rivers (low/high predation; river distances: low Guanapo-high Guanapo = 11.1 km, high Guanapo-high Aripo = 23.9 km, high Aripo-low Aripo = 6.6 km; three lines from high-predation Aripo and five from each of the other focal populations; 18 lines total). Each observation was of one line at one date but measured intensity on and death of multiple hosts for each line. This analysis included some lines maintained in the laboratory for less than 30 days, but these lines necessarily had fewer observations and thus did not influence the analysis as much as lines with more observations. For intensity (N=425 observations), we used predation regime, river and number of fish in the common garden at time of measurement (because Gyrodactylus spp. can move relatively freely among fish) as fixed effects. Parasite line and line-day (days the line had been in the lab) nested within parasite line were included as

random effects. We used log(intensity) as the response variable. For death rate (N=216), we used predation regime and river as the fixed effects with parasite line and line-day nested within line as random effects, a Tweedie error family and a log link function. The same analyses were used when determining the effect of predation regime on intensity (N=208) and host death rate (N=102) for known G. turnbulli lines. We compare the theoretical model to the mean of back transformed partial residuals of infected host death rate to control for non-focal predictors, such as line-day, to find the most representative estimate of death rate in each predation regime (similar results are found from predicting mean death rate from statistical model fits instead of using partial residuals).

To determine trait differences by species, we considered all wild lines that were identified to species in high-predation populations (including seven from rivers considered non-focal due to lack of high-predation versus low-predation comparisons). Three of these lines were G. bullatarudis and 11 were G. turnbulli. Because all three G. bullatarudis lines were from high-predation populations, we compared species differences only within that regime. Species identity was used as a predictor instead of predation regime but statistical models were otherwise identical to those for the effect of predation regime for intensity (N=345) and infected host death rate (N=177).

**Theoretical modelling.** We wrote a relatively simple, ordinary differential equation model that retains the key biology of the predator–prey/host–parasite system. In the model, predators are not limited by prey/host density (for example, because predators are generalists), allowing us to represent predation as a parameter (*P*) for simplicity instead of a state variable. Susceptible hosts (*S*) become infected (*I*) and can recover to an immune state (*R*) with waning immunity (Table 1 shows symbols, values and units):

$$\frac{dS}{dt} = \left[a - q(S+I+R)\right](S+I+R) - \left(d + \frac{Pc_1}{c}\right)S - cTIS + zR \qquad (1a)$$

$$\frac{dI}{dt} = cTIS - \left(d + \frac{Pc_1}{c}\right)I - \nu I - \gamma I \tag{1b}$$

$$\frac{dR}{dt} = \gamma I - \left(d + \frac{Pc_1}{c}\right)R - zR\tag{1c}$$

Susceptible hosts are born from all hosts with density dependent, per capita birth rate a-q(S+I+R) (that is, hosts grow logistically, equation (1a)). Hosts die at background rate d and from predation at rate  $Pc_1/c$  that decreases with the host shoaling rate (c; that P and c<sub>1</sub> together determine the strength of predation). Along with parasite transmissibility given contact (T), the rate of density dependent transmission from I to S depends on the host–host contact rate, dictated by shoaling rate. Recovered hosts also move back into the susceptible class as immunity wanes at rate z (average duration of immunity is 1/z).

Infected hosts (equation (1b)) suffer background mortality and predation (predation is not selective in this model) while suffering additional mortality due to virulence,  $\nu$ . If predation were selective, especially to remove the sickest hosts, the consumptive effects of predation would be even more likely to select against virulence. Thus, selective predation seems unlikely to alter our conclusion that shoaling rate drives virulence (Extended Data Fig. 3). Infected hosts recover with rate  $\gamma$  (equation (1c)). Recovered hosts suffer background mortality and predation while losing immunity over time.

We modelled parasite and host evolution via Adaptive Dynamics<sup>51</sup>. Biologically, parasite evolution is rendered more complex by the presence of multiple lines and two phenotypically similar species; host evolution is also complex because shoaling rate has important genetic and plastic components<sup>29</sup>. For both host and parasite, our model is agnostic regarding the basis of adaptation but simply examines competition between phenotypes based on fitness of a rare phenotype (that is, invasion analysis). Each phenotype corresponds to an asexual genotype in the model. Fitness when invading depends on the traits of the mutant (m) and resident genotypes (r) for parasites and is given by equation (2a) (note that  $I_{\rm m}$  cancels out of all terms):

$$\frac{1}{I_{\rm m}} \frac{dI_{\rm m}}{dt} = cT_{\rm m}S_{\rm r}^* - d - \frac{Pc_1}{c} - v_{\rm m} - \gamma + \sigma cT_{\rm m}I_{\rm r}^* - \sigma cT_{\rm r}I_{\rm r}^*$$
 (2a)

$$v_{\mathbf{i}} = k_1 T_{\mathbf{i}}^{k_2} \tag{2b}$$

The resident sets host densities at  $S_r$  and  $I_s$ , which depend on its traits,  $T_r$  and  $v_r$  (linked by the trade-off in equation (2b)). Mutant fitness depends on transmission to susceptible hosts, background death, predation, virulence, recovery and gains and losses due to superinfection (equation (2a)). In superinfection, parasites of one genotype take over a host already infected by another genotype. We assume that each genotype has the same probability of successful superinfection given transmission,  $\sigma$ . This assumption is probably conservative as the probability of successful superinfection is often expected to increase with virulence<sup>12</sup>, which could amplify the impact of multiple infections to select for higher virulence.

From parasite fitness when invading, we find the continuously stable strategy (CSS)<sup>31</sup> for parasite virulence; a CSS represents a trait value that can be reached by gradual trait changes but that cannot be invaded by rare phenotypes with slightly different traits.

For host fitness, we used the Next Generation Matrix technique  $^{52}$  that accounts for fitness within each class and the rates of movement between classes (Supplementary Information). In the model, host genotypes differ in their shoaling rates,  $c_i$ . An invading host genotype (shoaling rate  $c_m$ ) contacts the resident genotype ( $c_i$ ) at the geometric mean of the two contact rates square root of  $c_m c_r$  for the purposes of transmission and predation, equation (3), following Bonds et al. An invading genotype suffers crowding (-q term, equation (3a)) from all hosts. Neglecting evolutionarily stable curves that are not CSSs (because we did not find any), only intersections of a host CSS curve and parasite CSS curve (Fig. 4) can be a coevolutionary stable point (coCSS). We confirmed that a potential coCSS is indeed a coCSS with the strong convergence stability criterion  $^{53}$ .

$$\frac{dS_{\rm m}}{dt} = \left[a - q(H_{\rm r})\right](H_{\rm m}) - \left(d + \frac{Pc_1}{\sqrt{c_{\rm m}c_{\rm r}}}\right)()S_{\rm m} - \sqrt{c_{\rm m}c_{\rm r}}TI_{\rm r}S_{\rm m} + zR_{\rm m} \quad (3a)$$

$$\frac{dI_{\rm m}}{dt} = \sqrt{c_{\rm m}c_{\rm r}}TI_{\rm r}S_{\rm m} - \left(d + \frac{Pc_1}{\sqrt{c_{\rm m}c_{\rm r}}}\right)I_{\rm m} - \nu I_{\rm m} - \gamma I_{\rm m}$$
(3b)

$$\frac{dR_{\rm m}}{dt} = \gamma I_{\rm m} - \left(d + \frac{Pc_1}{\sqrt{c_{\rm m}c_{\rm r}}}\right) R_{\rm m} - z R_{\rm m} \tag{3c}$$

Note: H = S + I + R. In the second alternate model, the rate of predation on the resident is  $Pc_1/(c_r^x)$ , and predation on the mutant is  $Pc_1/(c_rc_m)^{x/2}$  where 0 < x. x > 1 indicates that protection from predation more than doubles when the shoaling rate doubles. x < 1 would mean that protection from predation less than doubles when the shoaling rate doubles.

We have empirical estimates of some, but not all, of the parameters of the eco-coevolutionary model. As such, we used a simple evolutionary algorithm (described below) to estimate all model parameters, using empirical parameter estimates and field estimates of model outputs (for example, prevalence) to fit the model to the data. Importantly, we provided only the parameters of the virulence-transmission trade-off to the model, not levels of virulence corresponding to our four focal populations. Thus, model virulence is free to evolve along the virulence-transmissibility trade-off however best fits the other data; instead, we used the virulence of our four focal populations to validate the model.

Many empirical estimates came from the literature (see below). We estimated maximum birth rate (a) from lifetime fecundity of guppies with high food  $^{54}$  in the laboratory. We estimated background mortality in the absence of parasites and predators (d) as the inverse of life expectancy in the laboratory  $^{54}$ . We estimated recovery rate ( $\gamma$ ) as the inverse of the time required for fish to clear infection in the laboratory  $^{55}$ . We estimated the rate at which immunity wanes (z) from the observation that fish were roughly half resistant (averaging across totally resistant, partially resistant and not resistant) 21 days after initial infection  $^{56}$ . Our trait measurements provided estimates for the trade-off parameters (Fig. 3c), given an estimate of d.

For parameters where we lacked estimates (importantly  $Pc_1$  (which acts as one parameter as c<sub>1</sub> simply converts units) in low- and high-predation populations and the superinfection parameter,  $\sigma$ ), we also fit the model's eco-coevolutionary outputs at low and high predation to estimates of such outcomes in the field. We converted recapture rates from a mark-recapture experiment<sup>57</sup> into instantaneous mortality rates to determine overall mortality rate in the field  $(d + Pc_1/c + pv)$  for both a high-predation population and a low-predation population. We found a transmission rate reasonable for low-predation populations ( $cT_{Low}$ ) by fitting transmission rate to peak prevalence and timing of peak prevalence found for low-predation Aripo guppies and parasites in a stream mesocosm58. We also used estimates of shoaling rate, prevalence and host density (analysis of shoaling rate, prevalence and host density are further described below). We were able to fit some outputs to estimates from low-predation populations, high-predation populations and the ratio of the two (representing the impact of changing predation regime). For others, we have estimates of only one of these three. This scheme weighs the model training towards quantities that are well characterized. Table 1 provides

We optimized the model's fit to both these empirical parameter estimates and field-estimated model outputs with a simple evolutionary algorithm . We began with parameters at their estimated values (for a, d,  $k_1$ ,  $k_2$ ,  $\gamma$  and z). Initial values of other parameters were chosen arbitrarily ( $q=1\times10^{-2}$ , ( $Pc_1$ ) $_{\rm Low}=1\times10^{-2}$ , ( $Pc_2$ ) $_{\rm Lin}=3\times10^{-2}$ ,  $\sigma=0.5$ ). Each parameter was mutated by a factor of  $10^x$ , where x is a single sample from the normal distribution N (0,0.05) to create a parameter set; each parameter set formed one strategy in the evolutionary algorithm. One un-mutated strategy and 299 mutated strategies were evaluated in one 'generation' of the algorithm by their summed relative error from all inputs and outputs with known estimates; summed relative error of strategy  $x=|a_x-a_{\rm data}|/a_{\rm data}+...+|cT_{\rm Low,x}-cT_{\rm Low,data}|/cT_{\rm Low,data}$ . There are four constrained parameters, four unconstrained parameters and eight independent scored outputs

(for example,  $p_{\text{Low}}$  is independent from  $p_{\text{Hi}}$  but not  $p_{\text{Hi}}/p_{\text{Low}}$ ). The strategy with the lowest summed relative error was passed to the next generation of the algorithm along with 299 mutated versions of itself. This process continues for 20 generations of the algorithm, as the model had asymptotically converged to a fit, yielding the parameter values used for the model (Table 1).

We performed a sensitivity analysis to determine how key outcomes responded to parameter values. We performed this analysis for coCSS parasite prevalence, host density, parasite virulence, host shoaling rate, overall host mortality, transmission rates and the ratios of these quantities between high- and low-predation populations. We also examine two other key 'proportion change metrics' representing how key factors change between the two focal predation levels. First was the proportion of total host mortality change with predation regime that is caused by increased parasite-induced mortality:  $(p_{Hi}v_{Hi} - p_{Low}v_{Low})$  $[(d+p_{Hi}v_{Hi}+P_{High}c_1/c_{Hi})-(d+p_{Low}v_{Low}+P_{Low}c_1/c_{Low})]$ . Second was the proportion of change in coevolutionary virulence across the predation regime that is via a predator's non-consumptive effects (evolution of higher shoaling rate). We defined this as the strength of pathway 3 (negative) plus the strength of pathway 4 (positive) divided by the summed strength of all pathways (Fig. 1); we averaged pathway strength at the low-predation point and the high-predation point together to get one strength for each pathway (code availability statement below). To generate random parameter sets, we used Latin Hypercube sampling with the 'lhs' R package<sup>60</sup> and then computed the partial rank correlation coefficients of the parameters with respect to each model outcome of interest (coevolutionary outcomes and key proportion change metrics) for 5 × 10<sup>3</sup> runs using the R package 'sensitivity'61. See Supplementary Fig. 2 and Supplementary Table 2 for results from the sensitivity analysis.

Field surveys of shoaling rate, prevalence and host density. In March 2020, we collected guppies from each of our four focal populations using seine nets, transported them to the field station and held them in pools (80 cm diameter) for 24h to 48h (mean = 33.6h) before assaying their shoaling tendency. We used a standard assay to assess the shoaling tendency of individual fish<sup>62</sup> and recorded each trial using GoPro cameras (HERO4). We allowed fish to acclimatize for 10 min before removing a partition separating the focal fish from a shoal tank (containing three non-focal individuals from the same population), waited 200 s after this removal and then recorded the proximity of the focal fish to the shoal for a further 10 min using Boris (v7.9.8) (ref. 63). All assays and behavioural recordings were conducted by a single observer blind to infection status and predation regime. We removed some fish from the analysis because of camera error or because the fish did not move for the trial duration. Our final sample sizes for each population were—low-predation Guanapo: 4 females, 5 males; high-predation: 3 females, 3 males; low-predation Aripo: 14 females, 13 males; high-predation: 12 females, 14 males. We recorded fish weight, length, sex and presence of Gyrodactylus spp. infection after its behaviour assay and tested for their effects, along with fish predation regime and river of origin, on % time shoaling using a generalized linear mixed model (Beta error, logit link function). Date of trial, lighting level and behaviour enclosure were included as random effects.

We collected prevalence estimates in March 2020 by catching between 50 and 30 fish per site with a  $1 \text{ m} \times 1 \text{ m}$  seine net and screening those from the Caroni drainage for parasites as above at a nearby field station.

We extracted estimates of shoaling rate, prevalence and host density from the literature (Supplementary Note provides more details) and supplemented them with our own, new data from field surveys of shoaling rate and prevalence. We used mixed models to test whether guppy shoaling behaviour, *Gyrodactylus* spp. prevalence and guppy density differed between predation regimes. In these models, we used predation regime as a fixed effect along with river and year as random effects. We included only rivers with paired estimates from high- and low-predation populations because of variation across rivers. Each population average for a given site + year was one data point in these analyses. For % time shoaling (22 estimates, 4 rivers<sup>28,64-60</sup>) and prevalence (107 estimates, 11 rivers<sup>30,33,57,58,67-69</sup>), we used a generalized linear mixed model beta regression with a logit link. For host density (23 estimates, 4 rivers<sup>70,73</sup>), we used a linear mixed model.

Animal use ethics statement. All collections and fish-handling protocols were approved by the University of Pittsburgh's Institutional Animal Care and Use Committee protocol 18072155 and 21069471. The permit to collect and export guppies was granted by the Director of Fisheries in the Ministry of Agriculture, Land and Fisheries Division, Aquaculture Unit of the Republic of Trinidad and Tobago on 26 February 2020 (copy available upon request). The US Import/Export License for live and preserved fish was issued by the US Fish and Wildlife Service, Office of Law Enforcement permit number A107080 on 21 February 2020 for the shipment of live guppies to the University of Pittsburgh. Samples were declared and cleared via Fish and Wildlife Service form 3-177 on 11 March 2020.

**Reporting Summary.** Further information on research design is available in the Nature Research Reporting Summary linked to this article.

#### Data availability

The data is available at https://doi.org/10.5061/dryad.k3j9kd59h.

#### Code availability

The code is available at https://doi.org/10.5061/dryad.k3j9kd59h.

Received: 20 October 2021; Accepted: 11 April 2022; Published online: 26 May 2022

#### References

- Everard, M., Johnston, P., Santillo, D. & Staddon, C. The role of ecosystems in mitigation and management of Covid-19 and other zoonoses. *Environ. Sci. Policy* 111, 7–17 (2020).
- Alizon, S., Hurford, A., Mideo, N. & Van Baalen, M. Virulence evolution and the trade-off hypothesis: history, current state of affairs and the future. *J. Evolut. Biol.* 22, 245–259 (2009).
- Cressler, C. E., McLeod, D. V., Rozins, C., Van Den Hoogen, J. & Day, T. The adaptive evolution of virulence: a review of theoretical predictions and empirical tests. *Parasitology* 143, 915–930 (2016).
- Acevedo, M. A., Dillemuth, F. P., Flick, A. J., Faldyn, M. J. & Elderd, B. D. Virulence-driven trade-offs in disease transmission: a meta-analysis. *Evolution* 73, 636–647 (2019).
- Anderson, R. M. & May, R. M. Coevolution of hosts and parasites. Parasitology 85, 411–426 (1982).
- McKay, B., Ebell, M., Dale, A. P., Shen, Y. & Handel, A. Virulence-mediated infectiousness and activity trade-offs and their impact on transmission potential of influenza patients. *Proc. R. Soc. B* 287, 20200496 (2020).
- Bonneaud, C. et al. Experimental evidence for stabilizing selection on virulence in a bacterial pathogen. Evol. Lett. 4, 491–501 (2020).
- De Roode, J. C., Yates, A. J. & Altizer, S. Virulence-transmission trade-offs and population divergence in virulence in a naturally occurring butterfly parasite. *Proc. Natl Acad. Sci. USA* 105, 7489–7494 (2008).
- Fraser, C., Hollingsworth, T. D., Chapman, R., de Wolf, F. & Hanage, W. P. Variation in HIV-1 set-point viral load: epidemiological analysis and an evolutionary hypothesis. *Proc. Natl Acad. Sci. USA* 104, 17441–17446 (2007).
- 10. Choo, K., Williams, P. D. & Day, T. Host mortality, predation and the evolution of parasite virulence. *Ecol. Lett.* **6**, 310–315 (2003).
- 11. Williams, P. D. & Day, T. Interactions between sources of mortality and the evolution of parasite virulence. *Proc. R. Soc. B* **268**, 2331–2337 (2001).
- 12. Gandon, S., Jansen, V. A. & Van Baalen, M. Host life history and the evolution of parasite virulence. *Evolution* **55**, 1056–1062 (2001).
- Prado, F., Sheih, A., West, J. D. & Kerr, B. Coevolutionary cycling of host sociality and pathogen virulence in contact networks. *J. Theor. Biol.* 261, 561–569 (2009).
- Herre, E. A. Population structure and the evolution of virulence in nematode parasites of fig wasps. Science 259, 1442–1445 (1993).
- Boots, M. & Mealor, M. Local interactions select for lower pathogen infectivity. Science 315, 1284–1286 (2007).
- 16. Alizon, S., de Roode, J. C. & Michalakis, Y. Multiple infections and the evolution of virulence. *Ecol. Lett.* 16, 556–567 (2013).
- Bull, J. J. & Lauring, A. S. Theory and empiricism in virulence evolution. PLoS Pathog. 10, e1004387 (2014).
- Brown, S. P., Hochberg, M. E. & Grenfell, B. T. Does multiple infection select for raised virulence? *Trends Microbiol.* 10, 401–405 (2002).
- Peacor, S. D. & Werner, E. E. The contribution of trait-mediated indirect effects to the net effects of a predator. *Proc. Natl Acad. Sci. USA* 98, 3904–3908 (2001).
- Seppälä, O., Karvonen, A. & Valtonen, E. T. Shoaling behaviour of fish under parasitism and predation risk. *Anim. Behav.* 75, 145–150 (2008).
- Lopez, L. K. & Duffy, M. A. Mechanisms by which predators mediate host-parasite interactions in aquatic systems. *Trends Parasitol.* 37, 890–906 (2021).
- Rigby, M. C. & Jokela, J. Predator avoidance and immune defence: costs and trade-offs in snails. Proc. R. Soc. B 267, 171–176 (2000).
- Krause, J., Ruxton, G. D., Ruxton, G. & Ruxton, I. G. Living in Groups (Oxford Univ. Press, 2002).
- Godin, J.-G. J. Antipredator function of shoaling in teleost fishes: a selective review. Nat. Can. 113, 241–250 (1986).
- Gandon, S., van Baalen, M. & Jansen, V. A. The evolution of parasite virulence, superinfection, and host resistance. Am. Nat. 159, 658–669 (2002).
- Magurran, A. E. Evolutionary Ecology: The Trinidadian Guppy (Oxford Univ. Press, 2005).
- Magurran, A. E. & Seghers, B. H. Variation in schooling and aggression amongst guppy (*Poecilia reticulata*) populations in Trinidad. *Behaviour* 118, 214–234 (1991).
- Seghers, B. H. & Magurran, A. E. Predator inspection behaviour covaries with schooling tendency amongst wild guppy, *Poecilia reticulata*, populations in Trinidad. *Behaviour* 128, 121–134 (1994).
- Huizinga, M., Ghalambor, C. & Reznick, D. The genetic and environmental basis of adaptive differences in shoaling behaviour among populations of Trinidadian guppies, *Poecilia reticulata*. J. Evolut. Biol. 22, 1860–1866 (2009).

- Stephenson, J. F., Van Oosterhout, C., Mohammed, R. S. & Cable, J. Parasites
  of Trinidadian guppies: evidence for sex- and age-specific trait-mediated
  indirect effects of predators. *Ecology* 96, 489–498 (2015).
- Richards, E. L., Van Oosterhout, C. & Cable, J. Sex-specific differences in shoaling affect parasite transmission in guppies. PLoS ONE 5, e13285 (2010).
- Johnson, M. B., Lafferty, K. D., Van Oosterhout, C. & Cable, J. Parasite transmission in social interacting hosts: monogenean epidemics in guppies. *PLoS ONE* https://doi.org/10.1371/journal.pone.0022634 (2011).
- 33. Gotanda, K. M. et al. Adding parasites to the guppy-predation story: insights from field surveys. *Oecologia* 172, 155–166 (2013).
- Fraser, B. A., Ramnarine, I. W. & Neff, B. D. Temporal variation at the MHC class IIB in wild populations of the guppy (*Poecilia reticulata*). Evolution 64, 2086–2096 (2010).
- Stephenson, J. F. et al. Host heterogeneity affects both parasite transmission to and fitness on subsequent hosts. *Philos. Trans. R. Soc. B* 372, 20160093 (2017).
- Cable, J. & Van Oosterhout, C. The impact of parasites on the life history evolution of guppies (*Poecilia reticulata*): the effects of host size on parasite virulence. *Int. J. Parasitol.* 37, 1449–1458 (2007).
- Reznick, D. N., Butler, M. J. IV, Rodd, F. H. & Ross, P. Life-history evolution in guppies (*Poecilia reticulata*) 6. Differential mortality as a mechanism for natural selection. *Evolution* 50, 1651–1660 (1996).
- Bonds, M. H., Keenan, D. C., Leidner, A. J. & Rohani, P. Higher disease prevalence can induce greater sociality: a game theoretic coevolutionary model. *Evolution* 59, 1859–1866 (2005).
- Kerr, B., Neuhauser, C., Bohannan, B. J. & Dean, A. M. Local migration promotes competitive restraint in a host–pathogen 'tragedy of the commons'. *Nature* 442, 75–78 (2006).
- Boots, M. & Sasaki, A. 'Small worlds' and the evolution of virulence: infection occurs locally and at a distance. Proc. R. Soc. B 266, 1933–1938 (1999).
- Wild, G., Gardner, A. & West, S. A. Adaptation and the evolution of parasite virulence in a connected world. *Nature* 459, 983–986 (2009).
- 42. Dargent, F., Rolshausen, G., Hendry, A., Scott, M. & Fussmann, G. Parting ways: parasite release in nature leads to sex-specific evolution of defence. *J. Evolut. Biol.* **29**, 23–34 (2016).
- Reznick, D. A., Bryga, H. & Endler, J. A. Experimentally induced life-history evolution in a natural population. *Nature* 346, 357–359 (1990).
- 44. Stephenson, J. F., van Oosterhout, C. & Cable, J. Pace of life, predators and parasites: predator-induced life-history evolution in Trinidadian guppies predicts decrease in parasite tolerance. *Biol. Lett.* 11, 20150806 (2015).
- Stephenson, J. F., Stevens, M., Troscianko, J. & Jokela, J. The size, symmetry, and color saturation of a male guppy's ornaments forecast his resistance to parasites. Am. Naturalist 196, 597–608 (2020).
- Godin, J.-G. J. & McDonough, H. E. Predator preference for brightly colored males in the guppy: a viability cost for a sexually selected trait. *Behav. Ecol.* 14, 194–200 (2003).
- 47. Van Oosterhout, C., Harris, P. & Cable, J. Marked variation in parasite resistance between two wild populations of the Trinidadian guppy, *Poecilia reticulata* (Pisces: Poeciliidae). *Biol. J. Linn. Soc.* **79**, 645–651 (2003).
- Hawley, D. M., Gibson, A. K., Townsend, A. K., Craft, M. E. & Stephenson, J. F. Bidirectional interactions between host social behaviour and parasites arise through ecological and evolutionary processes. *Parasitology* 148, 274–288 (2020).
- Janecka, M. J., Rovenolt, F. & Stephenson, J. F. How does host social behavior drive parasite non-selective evolution from the within-host to the landscape-scale? *Behav. Ecol. Sociobiol.* 75, 1–20 (2021).
- Tao, H., Li, L., White, M. C., Steel, J. & Lowen, A. C. Influenza A virus coinfection through transmission can support high levels of reassortment. J. Virol. 89, 8453–8461 (2015).
- 51. Eshel, I. Evolutionary and continuous stability. *J. Theor. Biol.* **103**, 99–111 (1983).
- Hurford, A., Cownden, D. & Day, T. Next-generation tools for evolutionary invasion analyses. J. R. Soc. Interface 7, 561–571 (2009).
- Leimar, O. Multidimensional convergence stability. Evolut. Ecol. Res. 11, 191–208 (2009).
- 54. Reznick, D., Bryant, M. & Holmes, D. The evolution of senescence and postreproductive lifespan in guppies (*Poecilia reticulata*). *PLoS Biol.* 4, e7 (2005).
- Stephenson, J. F. Parasite-induced plasticity in host social behaviour depends on sex and susceptibility. *Biol. Lett.* https://doi.org/10.1098/rsbl.2019.0557 (2019).
- Lopez, S. Acquired resistance affects male sexual display and female choice in guppies. Proc. R. Soc. B 265, 717–723 (1998).
- van Oosterhout, C. et al. Selection by parasites in spate conditions in wild Trinidadian guppies (*Poecilia reticulata*). Int. J. Parasitol. 37, 805–812 (2007).
- 58. Pérez-Jvostov, F., Hendry, A. P., Fussmann, G. F. & Scott, M. E. Are host-parasite interactions influenced by adaptation to predators? A test with guppies and *Gyrodactylus* in experimental stream channels. *Oecologia* 170, 77–88 (2012).

- Eiben, A. E. & Smith, J. E. Introduction to Evolutionary Computing (Springer, 2003).
- 60. Carnell, R. lhs: Latin hypercube samples v.1.1.1 (R-Project, 2020).
- Iooss, B., Da Veiga, S., Janon, A. & Pujol, G. Sensitivity: Global sensitivity analysis of model outputs v.1.25.0 (R-Project, 2021).
- Wright, D. & Krause, J. Repeated measures of shoaling tendency in zebrafish (*Danio rerio*) and other small teleost fishes. *Nat. Protoc.* 1, 1828–1831 (2006).
- Friard, O. & Gamba, M. BORIS: a free, versatile open-source event-logging software for video/audio coding and live observations. *Methods Ecol. Evol.* 7, 1325–1330 (2016).
- 64. Griffiths, S. W. & Magurran, A. E. Sex and schooling behaviour in the Trinidadian guppy. *Anim. Behav.* **56**, 689–693 (1998).
- Magurran, A., Seghers, B., Carvalho, G. & Shaw, P. Behavioural consequences of an artificial introduction of guppies (*Poecilia reticulata*) in N. Trinidad: evidence for the evolution of anti-predator behaviour in the wild. *Proc. R. Soc. B* 248, 117–122 (1992).
- 66. Sievers, C. et al. Reasons for the invasive success of a guppy (*Poecilia reticulata*) population in Trinidad. *PLoS ONE* 7, e38404 (2012).
- Mohammed, R. S. et al. Parasite diversity and ecology in a model species, the guppy (Poecilia reticulata) in Trinidad. R. Soc. Open Sci. 7, 191112 (2020).
- Lyles, A. M. Genetic Variation and Susceptibility to Parasites: Poeclia reticulata Infected with Gyrodactylus turnbulli. PhD dissertation, Princeton Univ. (1990).
- 69. Fraser, B. A. & Neff, B. D. Parasite mediated homogenizing selection at the MHC in guppies. *Genetica* **138**, 273 (2010).
- Reznick, D. & Endler, J. A. The impact of predation on life history evolution in Trinidadian guppies (*Poecilia reticulata*). *Evolution* 36, 160–177 (1982).
- El-Sabaawi, R. W. et al. Assessing the effects of guppy life history evolution on nutrient recycling: from experiments to the field. *Freshw. Biol.* 60, 590–601 (2015).
- Liley, N. & Luyten, P. Geographic variation in the sexual behaviour of the guppy, *Poecilia reticulata* (Peters). *Behaviour* 95, 164–179 (1985).
- Reznick, D. N. et al. Eco-evolutionary feedbacks predict the time course of rapid life-history evolution. Am. Nat. 194, 671–692 (2019).

#### Acknowledgements

We thank M. Ramlal, D. Reznick and E. Rudzki for assistance with fieldwork.

E. Calcaterra, L. Colgan, J. Jokela, M. Sackett and N. Tardent provided technical assistance with parasite genotyping. J. Jokela, A. McKay, C. van Oosterhout, M. Turcotte, K. A. Young and three anonymous reviewers made useful comments on an earlier version of this manuscript. National Science Foundation Division of Environmental Biology number 2010826 (J.C.W.), National Science Foundation Division of Environmental Biology number 2010741 (M.J.J.), National Science Foundation Division of Graduate Education number 1747452 (F.R.) and University of Pittsburgh Central Research Development Fund (J.F.S.) provided funding.

#### **Author contributions**

Conceptualization: J.E.S. and J.C.W. Theoretical modelling: J.C.W., C.E.C. and J.E.S. Data collection from literature: F.R. Sensitivity analysis: J.C.W. and F.R. Field collections: M.J.J., D.R.C., R.P. and R.S.M. Laboratory trait measurements: R.P., D.R.C., M.J.J., R.D.K. and J.E.S. Parasite molecular work: M.J.J., R.D.K. and M.K. Parasite genetic analysis: M.J.J. and M.K. Trait data analysis: J.C.W., D.R.C. and J.E.S. Density and prevalence data analysis: J.C.W. Funding acquisition: J.C.W., M.J.J., F.R. and J.E.S. Writing, original draft: J.C.W. and J.E.S. Writing, review and editing: J.C.W., M.J.J., D.R.C., R.D.K., F.R., R.P., R.S.M., M.K., C.E.C. and J.E.S.

#### Competing interests

The authors declare no competing interests.

#### **Additional information**

Extended data is available for this paper at https://doi.org/10.1038/s41559-022-01772-5.

**Supplementary information** The online version contains supplementary material available at https://doi.org/10.1038/s41559-022-01772-5.

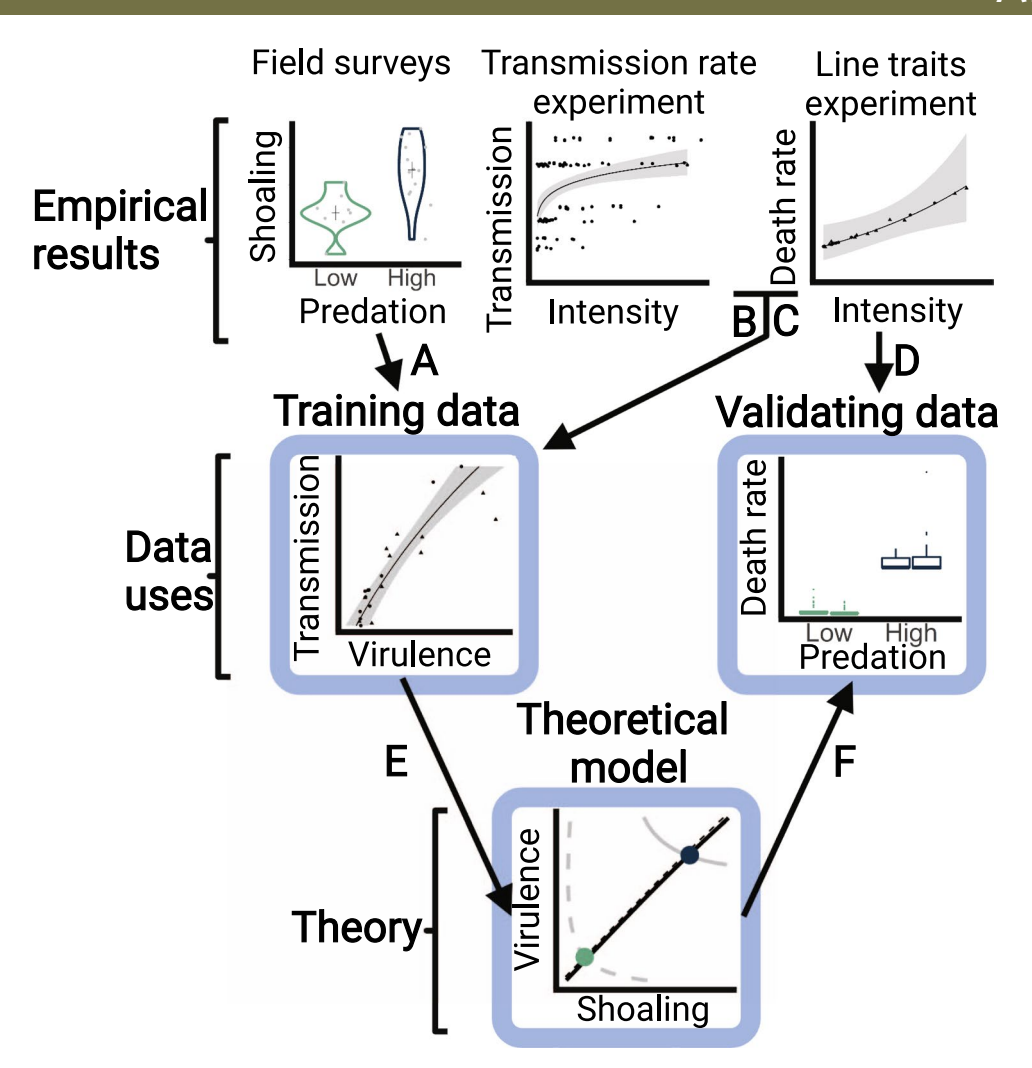
 $\textbf{Correspondence and requests for materials} \ \text{should be addressed to Jason C. Walsman}.$ 

**Peer review information** *Nature Ecology & Evolution* thanks Elisa Visher and the other, anonymous, reviewer(s) for their contribution to the peer review of this work. Peer reviewer reports are available.

Reprints and permissions information is available at www.nature.com/reprints.

**Publisher's note** Springer Nature remains neutral with regard to jurisdictional claims in published maps and institutional affiliations.

© The Author(s), under exclusive licence to Springer Nature Limited 2022

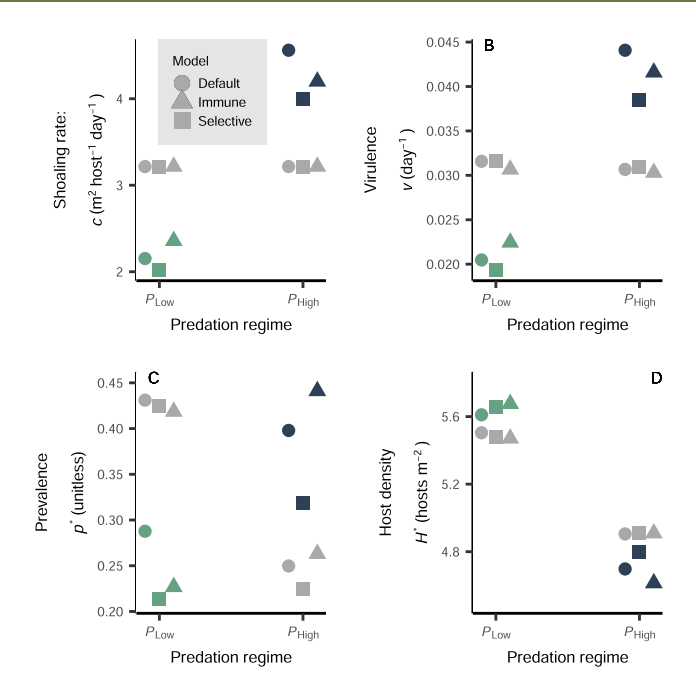


**Extended Data Fig. 1** | Flow of information between empirical results (row 1), data uses (row 2), and theory (row 3). (A) Much of the training data came from our field surveys, previously published surveys, and previously published laboratory data (see Fig. 5f-h for field surveys and see Table 1). (B) With our transmission rate experiment (and previously published data), we established the relationship between intensity and transmission rate (Fig. 3a). We connected these data to those from our line traits experiment, which link intensity and death rate (C; a measure of virulence shown in Fig. 3b). Together, these parameterize the transmission and virulence trade-off as training data (Fig. 3c). (D) The line traits experiment also provided validating data (Fig. 5i,j) on the average virulence and intensity of our four wild populations. (E) All training data, including the trade-off, was used to fit the theoretical model. (F) Once fit, the eco-coevolutionary model predicts where along the trade-off parasites should evolve (Figs. 4, 5d,e), predicting average virulence in the four populations of the validating data. Created with Biorender.com.

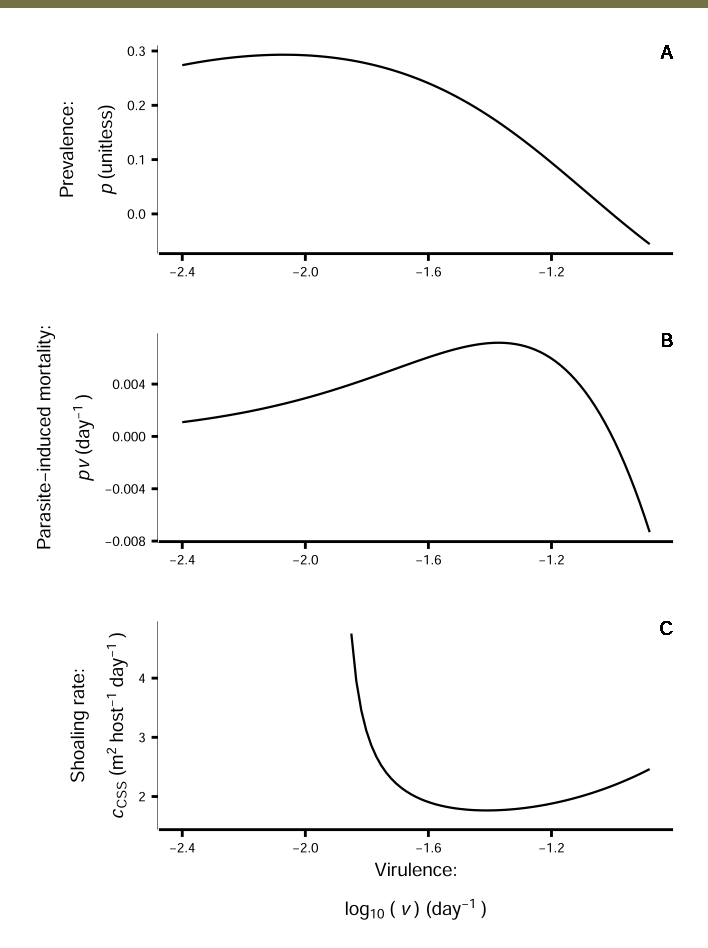
S	iite	Sa	mple size	% r	oure infecti	ons		%	coinfections		All int	fections
River	Predation	Fish	Worms/fish	G.t.	G.b.	Total	G.t.	G.b.	G.t.&G.b.	Total	% > 1 worm	% adjusted
			(mean±SE)									coinfection
Aripo	High	7	2.43±0.20	14.3	42.9	56.2	0	42.9	0	42.9	70.8	30.4
Aripo	Low	4	3.25±0.75	75	0	75	25	0	0	25	58.2	14.6
Guanapo	High	7	2.29±0.18	0	14.3	14.3	14.3	71.4	0	85.7	62.5	53.6
Guanapo	Low	5	2	60	20	80	20	0	0	20	61.9	12.4
Santa	High	7	4.86±1.30	0	0	0	0	71.4	28.6	100	92.6	92.6
Cruz												
Santa	Low	3	3±1	33.3	0	3.3	33.3	33.3	0	66.7	61.7	41.2
Cruz												

**Extended Data Fig. 2** | Data from field survey of coinfection rates in the wild. For each site (river+ predation regime), we genotyped a subset of worms from a sample of fish hosting more than one worm. We show the percent of infections that were pure (of either parasite species, light-yellow columns) and the total percent of pure infections (mid-blue column is sum of light-yellow columns). We also show the percent of coinfections that were multi-genotype coinfections of one species, the other, or contained both species (light pink columns). The sum of just the light pink columns gives the total rate of coinfection for fish infected with more than 1 worm (dark-purple column). The mid-blue and dark-purple columns must always sum to 100% in every row. We multiply the total coinfection rate (dark-purple; coinfections/infections with > 1) by the percentage of infections that have more than 1 worm to get the final, adjusted coinfection rate (coinfections/infections). See Supplementary Fig. 5 for a graphical example. G.t. = G. turnbulli and G.b. = G. bullatarudis.

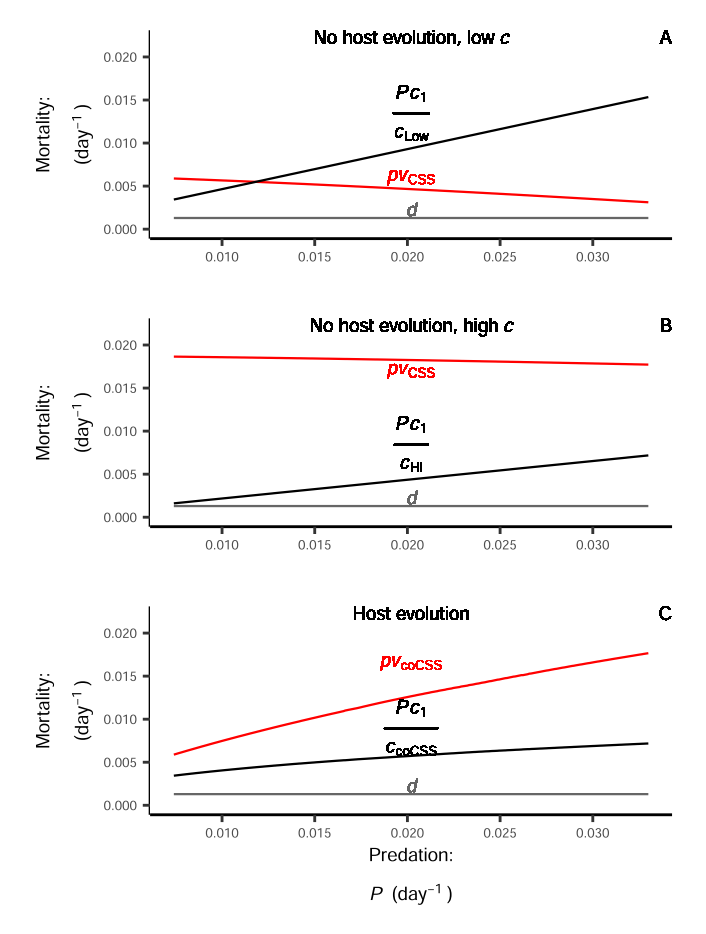
NATURE ECOLOGY & EVOLUTION ARTICLES



**Extended Data Fig. 3** | Neither selective predation nor variation in host immunity qualitatively alter key model outcomes. We compared the default model case (squares) to variations with selective predation (circles) or immune variation (triangles). We also compare outcomes with full coevolution at a given predation level (colour; *P* corresponding to Fig. 5) to outcomes without host evolution (grey). (**A**) Selective predation led to coevolution of lower shoaling rate. Increased immunity in low-predation populations led to coevolution of somewhat higher shoaling rate while decreased immunity in high-predation populations led to coevolution of somewhat lower shoaling rate. (**B**) Selective predation led to coevolution of lower virulence. Increased immunity in low-predation populations led to coevolution of higher virulence while decreased immunity in high-predation populations led to coevolution of lower virulence. For all models, increased virulence was driven by increased shoaling rate (compare colour points to grey). (**C**) Selective predation led to lower coevolutionary prevalence. Increased immunity led to lower coevolutionary prevalence while decreased immunity led to higher. (**D**) Selective predation led to higher coevolutionary host density. Increased immunity led to higher coevolutionary host density while decreased host density led to lower coevolutionary host density.



**Extended Data Fig. 4 | Virulence can select for increased shoaling rate.** Hosts can evolve increasing shoaling rate in response to increased virulence, especially at very high virulence (beyond range used in main text). (**A**) Increasing virulence (and transmissibility along the trade-off) can decrease prevalence. (**B**) Overall parasite-induced mortality can decrease if prevalence declines sharply enough. This decrease occurs because, while parasites are very virulent, very few hosts are infected and suffering that virulence. (**C**) At high virulence, increasing virulence can select for higher host shoaling rates. Parameters used: *c* = 2 used for (A) and (B); *P* = 0.074 used for (C). All other parameters at default (Table 1).



**Extended Data Fig. 5 | Host evolution in response to increasing predation causes parasite-induced mortality (red curves) to increase more than predator-induced mortality (black curves).** (**A**) Without host evolution (shoaling rate, *c*, set to the green point in Fig. 4 while parasites evolve to some CSS), parasite-induced mortality declines with predation while predator-induced mortality increases. Death from background sources (*d*, grey line) does not change. (**B**) This trend is similar for a higher *c* (set to high, blue point in Fig. 4). (**C**) When hosts evolve increasing *c* with increasing predation (coCSS curve connecting green and blue points in Fig. 4), parasite-induced mortality increases more than predator-induced mortality. This pattern is due to host evolution and is qualitatively unchanged if hosts evolve but parasites do not.

## nature portfolio

Walsman, Jason Janecka, Mary J Clark, David R Kramp, Rachael D Rovenolt, Faith Patrick, Regina Mohammed, Ryan S Konczal, Mateusz Cressler, Clayton E

Corresponding author(s): Stephenson, Jessica F

Last updated by author(s): Mar 17, 2022

### **Reporting Summary**

Nature Portfolio wishes to improve the reproducibility of the work that we publish. This form provides structure for consistency and transparency in reporting. For further information on Nature Portfolio policies, see our <u>Editorial Policies</u> and the <u>Editorial Policy Checklist</u>.

#### Statistics

For	all st	atistical analyses, confirm that the following items are present in the figure legend, table legend, main text, or Methods section.
n/a	Cor	nfirmed
	$\boxtimes$	The exact sample size (n) for each experimental group/condition, given as a discrete number and unit of measurement
	$\boxtimes$	A statement on whether measurements were taken from distinct samples or whether the same sample was measured repeatedly
	$\boxtimes$	The statistical test(s) used AND whether they are one- or two-sided  Only common tests should be described solely by name; describe more complex techniques in the Methods section.
	$\boxtimes$	A description of all covariates tested
	$\boxtimes$	A description of any assumptions or corrections, such as tests of normality and adjustment for multiple comparisons
$\boxtimes$		A full description of the statistical parameters including central tendency (e.g. means) or other basic estimates (e.g. regression coefficient) AND variation (e.g. standard deviation) or associated estimates of uncertainty (e.g. confidence intervals)
	$\boxtimes$	For null hypothesis testing, the test statistic (e.g. <i>F</i> , <i>t</i> , <i>r</i> ) with confidence intervals, effect sizes, degrees of freedom and <i>P</i> value noted <i>Give P values as exact values whenever suitable.</i>
$\boxtimes$		For Bayesian analysis, information on the choice of priors and Markov chain Monte Carlo settings
$\times$		For hierarchical and complex designs, identification of the appropriate level for tests and full reporting of outcomes
	$\boxtimes$	Estimates of effect sizes (e.g. Cohen's d, Pearson's r), indicating how they were calculated
		Our web collection on <u>statistics for biologists</u> contains articles on many of the points above.

#### Software and code

Policy information about availability of computer code

Data collection

R 4.0.3 was used for theoretical modelling. The code is provided in the SI and on Dryad (see Code Availability).

R 4.0.3 was used for data analysis. The code is provided in the SI and on Dryad (see Code Availability).

For manuscripts utilizing custom algorithms or software that are central to the research but not yet described in published literature, software must be made available to editors and reviewers. We strongly encourage code deposition in a community repository (e.g. GitHub). See the Nature Portfolio guidelines for submitting code & software for further information.

#### Data

Policy information about availability of data

All manuscripts must include a data availability statement. This statement should provide the following information, where applicable:

- Accession codes, unique identifiers, or web links for publicly available datasets
- A description of any restrictions on data availability
- For clinical datasets or third party data, please ensure that the statement adheres to our policy

Provide your data availability statement here.

## Field-specific reporting

Please select the one below that is the best fit for your research. If you are not sure, read the appropriate sections before making your selection.

Life sciences Behavioural & social sciences Ecological, evolutionary & environmental sciences

For a reference copy of the document with all sections, see <u>nature.com/documents/nr-reporting-summary-flat.pdf</u>

## Ecological, evolutionary & environmental sciences study design

All studies must disclose on these points even when the disclosure is negative.

Study description

- 1. We measured days until transmission of worm infection on a single donor-recipient pair of hosts as a function of the number of worms on the donor.
- 2. We measured the mortality imposed by worm infection and the number of worms per infected fish on various worm lines. Using the transmission-worm number relationship found in (1), this allowed us to find a trade-off between the mortality imposed by a worm line and its transmission rate.
- 3. Using parameters estimated in our focal system, we made a theoretical model of worm evolution along this trade-off as worms coevolved with fish hosts.
- 4. We collected wild fish hosts to assay their infections with worms, measure their behavior, test worm genetics, and found some of the worm lines for the trait measurements in (2). These collections also tested the model in (3).

See manuscript for more details.

Research sample

Wild collections involved fish hosts (Poecilia reticulata) of both sexes and all ages. Laboratory measurements employed adult hosts of both sexes as it is difficult to grow worm parasites on juvenile fish. In general, all conditions were kept as uniform as possible.

Sampling strategy

Sample sizes were not pre-calculated. Instead, the authors obtained the largest sample sizes possible given specimen availability and a viable quantity of effort. The authors believe the resulting sample sizes (listed in the manuscript) are sufficient, ranging from 22 populations at the fewest to over a thousand measurements on individual fish.

Data collection

Data was collected by the authors as described in the author contributions statement. Data for (1) was collected by counting worms on fish and checking recipient worms for infection every day. Data for (2) was collected by housing groups of infected fish, frequently counting the number of worms on fish and checking for fish death. We did not mark individual fish as preliminary data suggests this may influence infection dynamics; since housing social fish individually is also stressful, we were not able to control for repeated measurements of worm number on the same fish. However, the authors believe that the number of repeated measurements on each fish (approximately 5) is small compared to the overall sample size for this dataset (hundreds or thousands, depending on the subset of the data). Data for (4) was collected by capturing wild fish, counting their parasites at a field station, measuring their behavior at a field station, and sending live specimens back to the laboratory.

See manuscript for further details.

Timing and spatial scale

Samples for (1) were collected every day from October 1st, 2019 through October 5th, 2019. Samples for (2) were collected every few days from December 13th, 2019 until July 23rd, 2020. Samples for (4) were collected from late February of 2020, to late March of 2020.

Data exclusions

Analysis of average traits of worm lines in (2) treated each line as a data point of equal weight. Some lines went extinct in the lab very quickly (after 30 days or fewer). These lines' average traits were excluded from the analysis in (2) as they would be likely to introduce a high degree of variability. This criterion was not pre-established before data collection but was before data analysis.

Reproducibility

(1) was essentially a repeat of a previously-published experiment and found very similar results so data from the two experiments were analyzed together for greater power. There were no attempts to reproduce (2) and (4).

Randomization

Fish from a standardized genetic background were assigned randomly to host worms for (1) and (2). Each worm line was assigned randomly to a single tank.

Blinding

For (1), sample collectors were not aware of worm numbers when assaying transmission and vice versa. Sample collectors were not blinded for (2). For (4), sample collectors were not blinded because samples were processed as quickly as possible after collection on

	site.
Did the study involve fiel	d work? 🔀 Yes 🗌 No
Field work, collec	tion and transport
Field conditions	Fish and parasites were collected in Trinidad over a three-week period in late February and early March of 2020. Collections coincided with the dry season to ensure site accessibility. Weather conditions were clear, with mean ambient temperature near 29 degrees C. No substantial precipitation occurred during this period. Water temperature of collection sites ranged from 23 to 28 degrees C.
Location	Samples were collected at sites across rivers on the Northern and Southern Slopes of Trinidad's Northern mountain range (Caroni and Oropouche drainage and Marianne River on the northern slope) (Figure 1). Elevation for high predation sampling locations ranged in elevation from 200 to 300 feet above sea level. Elevation for low predation locations ranged from 600 to 1000 ft above sea level. Water depth for sampling sites ranged from 15 to 55 cm.
Access & import/export	Site accessibility varied widely. Some sites, especially in the lower courses were accessible via river-highway crossings. These sites required a short walk from the vehicle to the river. Other sites, especially in the upper courses were accessible via selecting a river access point and hiking upstream. All collections and fish handling protocols were approved by IACUC protocol 18072155 and 21069471 by the corresponding author's institution. The permit to collect and export guppies was granted by the Director of Fisheries in the Ministry of Agriculture, Land and Fisheries Division, Aquaculture Unit of the Republic of Trinidad and Tobago on 2/26/2020 (copy of the permit available on request). The United States Import/Export License for live and preserved fish was issued by the U.S. Fish and Wildlife Service, Office of Law Enforcement Permit number A107080 on 2/21/2020 for the shipment of live guppies to the corresponding author's institution. Preserved samples for genotyping were stored in 70% ethanol. All samples were declared and cleared via USFWS form 3-177 on 03/11/2020. At the corresponding author's institution, the samples remained in ethanol but were placed in a -20 C freezer.
Disturbance	Sample sites were selected to coincide with large, stable guppy populations to minimize disturbance.

## Reporting for specific materials, systems and methods

We require information from authors about some types of materials, experimental systems and methods used in many studies. Here, indicate whether each material, system or method listed is relevant to your study. If you are not sure if a list item applies to your research, read the appropriate section before selecting a response.

Materials & experimental systems		Methods			
n/a	Involved in the study	n/a	Involved in the study		
$\boxtimes$	Antibodies	$\boxtimes$	ChIP-seq		
$\boxtimes$	Eukaryotic cell lines	$\boxtimes$	Flow cytometry		
$\boxtimes$	Palaeontology and archaeology	$\boxtimes$	MRI-based neuroimaging		
	Animals and other organisms				
$\boxtimes$	Human research participants				
$\boxtimes$	Clinical data				
$\boxtimes$	Dual use research of concern				

#### Animals and other organisms

Policy information about studies involving animals; ARRIVE guidelines recommended for reporting animal research

Laboratory animals Poecilia reticulata, Gyrodactylus turnbulli, and Gyrodactylus bullatarudis.

Wild animals

Wild-caught animals were relatively uniform with respect to age and sex. Live fish and their worms were transported from Trinidad to the corresponding author's institution. After use in the study, fish and worms were used to found lines maintained in the laboratory for future studies.

Field-collected samples Field-collected samples were housed in 1.8 L tanks on a recirculating system (Aquaneering Inc.; 12L:12D; 24°C).

Ethics oversight The Institutional Animal Care and Use Committee at the corresponding author's institution provided ethical oversight and guidance on the use of animals.

Note that full information on the approval of the study protocol must also be provided in the manuscript.